

A Small Family of *MYB*-Regulatory Genes Controls Floral Pigmentation Intensity and Patterning in the Genus *Antirrhinum* ^W

Kathy Schwinn,^a Julien Venail,^b Yongjin Shang,^{a,c} Steve Mackay,^b Vibeke Alm,^{b,1} Eugenio Butelli,^b Ryan Oyama,^{b,2} Paul Bailey,^b Kevin Davies,^a and Cathie Martin^{b,3}

^aNew Zealand Institute for Crop and Food Research Limited, Private Bag 11600, Palmerston North, New Zealand

^bDepartment of Cell and Developmental Biology, John Innes Centre, Norwich Research Park, Colney, Norwich NR4 7UH, United Kingdom

^cInstitute of Molecular Biosciences, Massey University, Private Bag 11222, Palmerston North, New Zealand

The *Rosea1*, *Rosea2*, and *Venosa* genes encode MYB-related transcription factors active in the flowers of *Antirrhinum majus*. Analysis of mutant phenotypes shows that these genes control the intensity and pattern of magenta anthocyanin pigmentation in flowers. Despite the structural similarity of these regulatory proteins, they influence the expression of target genes encoding the enzymes of anthocyanin biosynthesis with different specificities. Consequently, they are not equivalent biochemically in their activities. Different species of the genus *Antirrhinum*, native to Spain and Portugal, show striking differences in their patterns and intensities of floral pigmentation. Differences in anthocyanin pigmentation between at least six species are attributable to variations in the activity of the *Rosea* and *Venosa* loci. Set in the context of our understanding of the regulation of anthocyanin production in other genera, the activity of *MYB*-related genes is probably a primary cause of natural variation in anthocyanin pigmentation in plants.

INTRODUCTION

Some of the most striking features of insect-pollinated flowering plants are their highly distinctive patterns of floral pigmentation. Many color patterns provide honey guides that direct pollinators toward the reproductive organs and the source of nectar within the flowers (Waser and Price, 1983). In *Antirrhinum majus*, color patterning results from the localized production of yellow aurone pigment in the hinge region created by the ventral and lateral petals of the corolla. The yellow is surrounded by magenta anthocyanin, which is produced more or less evenly in both inner and outer epidermal layers of the corolla lobes and at somewhat lower levels in the epidermal layers of the corolla tube (Figures 1A and 1J) (Jackson et al., 1992). This arrangement of yellow (aurone) and magenta (cyanidin) pigments provides a visual target for prospective pollinating bumblebees and probably guides them to the mouth of the fused corolla (Harbourne and

Smith, 1978; Penny, 1983; Lunau et al., 1996). Some natural isolates of *A. majus* have additional patterning, in the form of increased pigmentation in regions of the epidermis overlying the vascular strands of the petal (Baur, 1910a, 1910b; Kuckuck and Schick, 1930; Stubbe, 1966). This venal pattern of pigmentation predominates on the inner (adaxial) epidermis of the dorsal petal lobes but continues into the inner epidermis of the corolla tube and, in contrast with the UV light-absorbing flavonoids, probably provides additional visual guides for the bees once they enter the corolla tubes (Thompson et al., 1972; Lunau et al., 1996).

Europe hosts 20 distinct species of *Antirrhinum*, which are native to Spain, Portugal, France, and Italy (Sutton, 1988). Considerable variations in color pattern exist between species. Most are acyanic, or very palely pigmented with anthocyanin, although several of the palely pigmented species exhibit the strong venal pattern of pigmentation also observed in some isolates of *A. majus*. Some species also have enlarged zones of aurone accumulation, rendering the corolla lobes entirely yellow. This diversity in floral pigmentation patterning is diagnostic of the different species of *Antirrhinum* and is often used in their classification (Sutton, 1988). Flower color intensity and patterning may be traits that contribute significantly to pollinator selection in *Antirrhinum* and possibly also to reproductive isolation and speciation (Hodges and Arnold, 1994; Oyama, 2002).

A number of loci control anthocyanin production in flowers of the model species, *A. majus*. Mutations that affect the activity of structural genes encoding the enzymes of anthocyanin biosynthesis are well characterized and include mutations in the genes encoding chalcone synthase (*nivea*; *CHS*) (Sommer and Saedler, 1986), flavanone 3-hydroxylase (*incolorata*; *F3H*) (Martin et al.,

¹ Current address: Department of Molecular Biosciences, University of Oslo, P.O. Box 1041, Blindern, 0316 Oslo, Norway.

² Current address: Max-Planck-Institut für Chemische Ökologie, Hans-Knöll Strasse 8, 07745 Jena, Germany.

³ To whom correspondence should be addressed. E-mail cathie.martin@bbsrc.ac.uk; fax 44-1603-450045.

The author responsible for distribution of materials integral to the findings presented in this article in accordance with the policy described in the Instructions for Authors (www.plantcell.org) is: Cathie Martin (cathie.martin@bbsrc.ac.uk).

^WOnline version contains Web-only data.

Article, publication date, and citation information can be found at www.plantcell.org/cgi/doi/10.1105/tpc.105.039255.

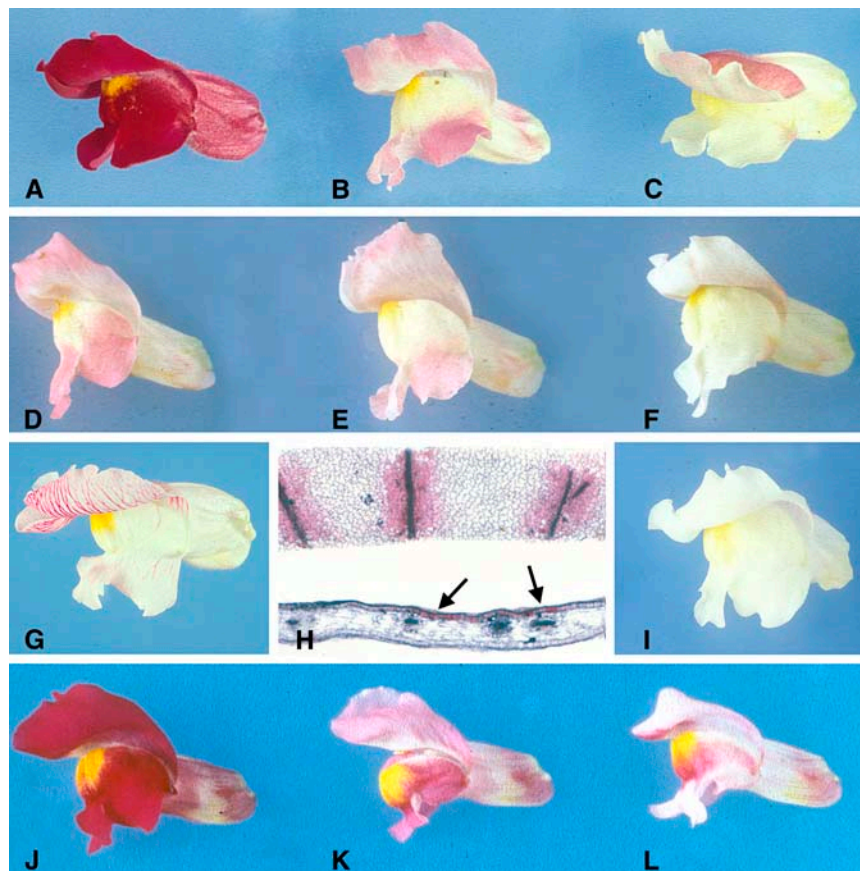


Figure 1. Floral Phenotypes of Regulatory Mutants of *A. majus*.

(A) Wild type.

(B) *ros^{col}* (grown outside).

(C) *ros^{dor}* (grown outside).

(D) to (F) Phenotypes of individuals in the F2 population of *ros^{col}* × *ros^{dor}*.

(D) *ros^{col}* homozygote.

(E) *ros^{col} ros^{dor}* heterozygote.

(F) *ros^{dor}* homozygote.

(G) *ros^{dor} Ve⁺*.

(H) Surface view and transverse section of a dorsal petal from a *ros^{dor} Ve⁺* individual. Arrows indicate the anthocyanin in the epidermal layer in regions overlying the vascular tissue.

(I) *ros^{dor}* grown in the greenhouse.

(J) to (L) Phenotypes of individuals in the F2 population of *eluta* (wild type) × *Eluta*.

(J) *eluta* (wild type) homozygote.

(K) *Eluta eluta* heterozygote.

(L) *Eluta* homozygote.

1991), dihydroflavonol 4-reductase (*pallida*; *DFR*) (Martin et al., 1985), anthocyanidin synthase (*candica*; *ANS*) (Martin et al., 1991), and flavonoid 3'-hydroxylase (*eosinea*; *F3'H*) (Stickland and Harrison, 1974). Generally, knockout mutations at these loci give rise to acyanic flowers or, in the case of *eosinea*, flowers that produce alternative types of anthocyanin. Some mutations of these genes can give rise to patterned alleles (Coen et al., 1986; Martin et al., 1987; Coen and Carpenter, 1988; Martin and Lister, 1989), but patterned phenotypes invariably result from alleles in which the regulation of the expression of the structural gene has been affected, either through changes to the regulatory motifs of

the promoters of the structural genes or through likely production of small interfering RNAs (Coen et al., 1986; Martin et al., 1987; Coen and Carpenter, 1988; Almeida et al., 1989; Martin and Lister, 1989; Robbins et al., 1989; Bollmann et al., 1991; Della Vedova et al., 2005). A number of mutations that affect the activity of regulatory genes that control the expression of the structural genes of floral pigment production have also been described, including *delila* (*del*), *Eluta* (*El*), *rosea* (*ros*), *Venosa* (*Ve*), and *mutabilis* (*mut*) (Wheldale, 1907; Baur, 1910a, 1910b; Kuckuck and Schick, 1930; Stubbe, 1966). Mutations in the regulatory genes do not abolish pigmentation but change the

pattern of pigmentation within the flowers: *Delila* affects pigmentation in the corolla tube; *Mut* affects pigmentation in the corolla lobes; *Rosea* affects the pattern and intensity of pigmentation in both lobes and tubes; and *Venosa* affects pigmentation of the epidermis overlying the veins in both lobes and tubes. Of the regulatory genes, only *Delila* has been characterized molecularly and shown to encode a basic helix-loop-helix (bHLH) transcription factor that is required for the activation of expression of the late biosynthetic genes (including *F3H*, *DFR*, *AS*, and UDP-glucose 3-O-flavonoid transferase [*UFGT*]) in the corolla tube (Martin et al., 1991; Goodrich et al., 1992; Martin and Gerats, 1993). The other regulatory loci also influence the levels of transcripts of the biosynthetic genes active late in the anthocyanin biosynthetic pathway for their control of pigment patterning (Martin et al., 1991; Schwinn, 1999).

In maize (*Zea mays*), it has been shown that two types of transcription factor, a MYB-related protein and a bHLH-containing protein, interact to activate genes in the anthocyanin biosynthetic pathway (Cone et al., 1986, 1993; Paz-Ares et al., 1986, 1987; Chandler et al., 1989; Ludwig et al., 1989; Consonni et al., 1992, 1993; Goff et al., 1992; Sainz et al., 1997b; Zimmermann et al., 2004). In different accessions of maize, the genes encoding these proteins have been variously amplified, such that genes encoding functionally equivalent proteins are active in different tissues of the vegetative and reproductive phases of growth (Chandler et al., 1989; Cone et al., 1993; Piliu et al., 2003). Some of the resultant variation in plant pigment patterning may be attributable to human selection for more exotic pigmentation forms, because such lines were highly prized by the indigenous peoples of Central America (Lonnig and Saedler, 1997). In maize, an additional gene, *pac1*, encodes a WD repeat protein that affects the levels of anthocyanin production in kernels (Carey et al., 2004). By analogy to the activity of the homologous protein TRANSPARENT TESTA GLABRA1 (TTG1) in *Arabidopsis thaliana* (Walker et al., 1999), it seems likely that WD repeat proteins stabilize the interaction between MYB and bHLH proteins and so promote the transcriptional activation of the structural genes of the anthocyanin biosynthetic pathway (Serna, 2004; Zimmermann et al., 2004; Broun, 2005; Ramsay and Glover, 2005; Lepiniec et al., 2006).

In *A. majus*, the molecular characterization of *delila* demonstrated that gene products similar to those in maize regulate anthocyanin production in dicotyledonous species (Goodrich et al., 1992). This has also been shown to be the case for flowers of other dicotyledonous species such as morning glory (*Ipomoea purpurea*, *Ipomoea tricolor*) (Park et al., 2004; Chang et al., 2005), in vegetative tissues of *Perilla frutescens* (Gong et al., 1999; Sompornpailin et al., 2002; Springob et al., 2003), and in *Petunia*, in which a MYB-related gene, *AN2*, is required for anthocyanin production in flowers (Quattrocchio, 1994; Quattrocchio et al., 1999) and a bHLH protein, *AN1*, interacts with *AN2* to activate anthocyanin biosynthesis (Spelt et al., 2000). A second gene encodes another bHLH protein, *JAF13*, which also interacts with *AN2*, but *JAF13* is not able to complement *an1* mutants and so is unlikely to be involved directly in regulating the transcription of anthocyanin biosynthetic genes (Quattrocchio et al., 1998; Spelt et al., 2000). It has been suggested that *AN2* activates the expression of *AN1* (Spelt et al., 2000). The *AN2* MYB protein is

thought to interact with *AN1* to activate anthocyanin biosynthetic gene expression in conjunction with *AN11*, a WD repeat protein structurally similar to *pac1* and *TTG1* (de Vetten et al., 1997). Mutants of *AN2* still synthesize anthocyanins in the corolla tubes and the limb retains pale pigmentation, which has led to the suggestion that other genes encoding R2R3 MYB proteins structurally related to *AN2* also contribute to the regulation of anthocyanin biosynthesis in *Petunia* flowers. One possible candidate is the *AN4* gene (Spelt et al., 2000; Koes et al., 2005).

We have characterized the activity of three genes encoding MYB-related transcription factors active in the flowers of *A. majus*. Analysis of mutant phenotypes showed that these genes contribute to the intensity and pattern of anthocyanin production in flowers. Despite the close structural similarity of these regulatory proteins, analysis of mutants showed that they influence the expression of target genes encoding the enzymes of anthocyanin biosynthesis with different specificities. Consequently, they are not precisely equivalent, biochemically, in their activities. Different species of the genus *Antirrhinum*, native to Spain and Portugal, show striking differences in their patterns and intensities of floral pigmentation. The differences in anthocyanin production between the six species investigated are attributable to variations in the activity of the *Rosea* and *Venosa* loci encoding these MYB-related regulatory proteins. Set in the context of our understanding of the regulation of anthocyanin production in other genera, the activity of MYB-related genes is probably a primary cause of natural variation in this trait in plants.

RESULTS

Phenotypes of the *rosea* and *venosa* Mutants Affecting Floral Pigmentation Intensity and Patterning

There are two extant mutant alleles of the *rosea* locus of *A. majus* called *rosea^{colorata}* (*ros^{col}*) (Figure 1B) and *rosea^{dorsea}* (*ros^{dor}*) (Figure 1C) (Baur, 1910a; Stubbe, 1966). Wild-type (*Ros⁺*) flowers are almost completely self-colored, with high levels of red/magenta anthocyanin produced in both lobes and tubes of the corolla. Only the central region of the fused ventral and lateral petals is colored yellow, as a result of the accumulation of aurone in the absence of anthocyanin (Figure 1A). The vegetative parts of the plant also accumulate anthocyanin, including leaves (especially in the cells of the ventral [abaxial] epidermis) and stems.

Both *rosea* mutants have paler floral pigmentation. *ros^{col}* has weak anthocyanin production restricted to the inner epidermis of the petals and a ring of pigment at the base of the corolla tube (Figure 1B). There is no anthocyanin pigment produced in the stems of the plant, although the abaxial surfaces of the leaves accumulate anthocyanin in field-grown plants. *ros^{dor}* has flowers that have a weak ring of anthocyanin production toward the base of the tube and anthocyanin accumulation on the outer epidermis of the dorsal lobes (Figure 1C). The floral pigmentation in *ros^{dor}* is very dependent on environmental conditions. At the higher temperatures (25°C) and lower light levels typical of greenhouses in the United Kingdom, no pigment is produced in the lobes (Figure 1I). Under the higher light but lower temperatures outside, field-grown *ros^{dor}* plants have prominent pigmentation on their dorsal lobes (Figure 1C). The vegetative parts of *ros^{dor}* plants are

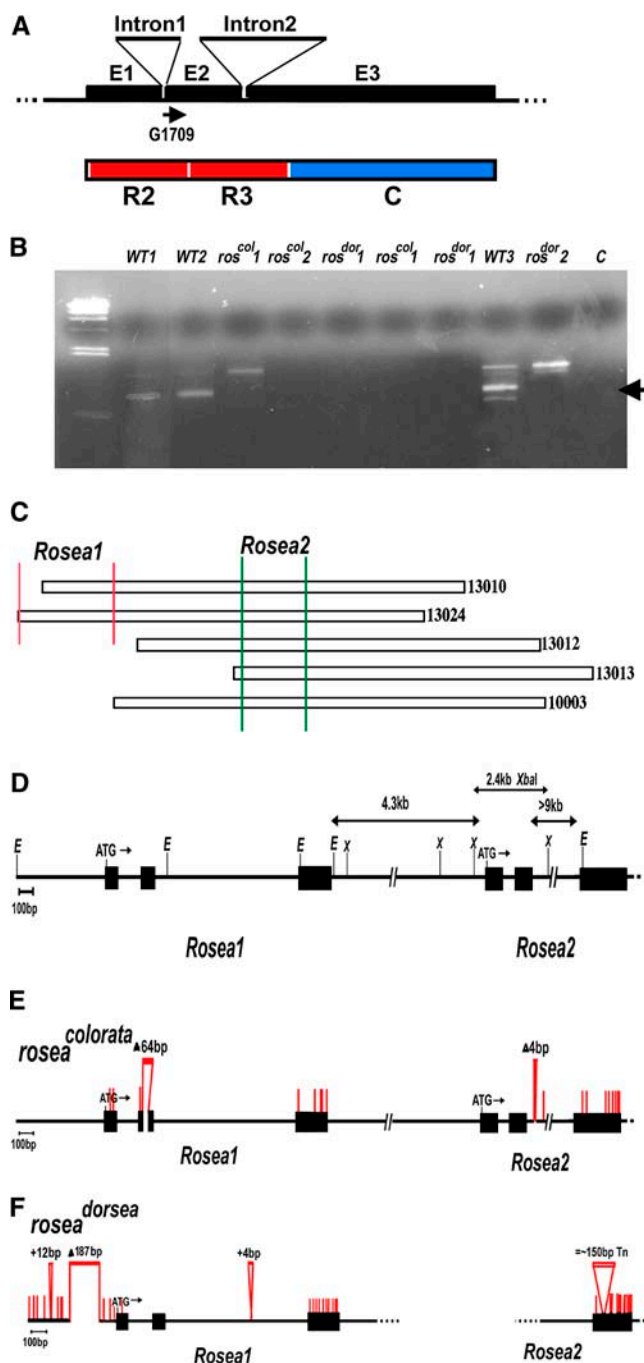


Figure 2. Structure of the *Rosea* Locus in Wild-Type *A. majus* and in *ros^{col}* and *ros^{dor}* Mutants.

(A) Scheme of the gene structure of members of the R2R3 MYB subgroup 6 family (Kranz et al., 1998). The intron positions are conserved between monocots and dicots. Below the line, a scheme of the encoded R2R3 MYB proteins is shown aligned to the exons (E1 to E3). R2 and R3 indicate the MYB repeats most similar to the second and third repeats of the prototypic MYB protein, c-Myb, respectively. C indicates the C-terminal domain. The position of the sequence in oligonucleotide G1709 is indicated by an arrow.

(B) Ethidium bromide-stained agarose gel showing PCR products of 3'

darkly pigmented, including stems and leaves. The mutations are fully recessive to the wild-type *Ros⁺* allele. Furthermore, crosses between *ros^{col}* and *ros^{dor}* do not complement (Figures 1D to 1F). F1 plants have flowers with an intermediate phenotype between the two alleles, indicating that they carry mutations at the same locus.

The phenotype conferred by *Venosa* (*Ve⁺*) in *A. majus* involves the production of magenta anthocyanin pigment in tissue over the veins of the corolla (Figure 1G) (Baur, 1910a; Kuckuck and Schick, 1930; Stubbe, 1966). Pigment production is limited to the inner epidermis of the petal lobes and to the inner epidermis of the corolla tube (Figure 1H). The phenotype of *Ve⁺* is not apparent in wild-type *A. majus* because the strong self-color masks the venal patterning. However, the phenotype is clear in the *ros^{dor}* and *ros^{col}* backgrounds (i.e., *Ros⁺* is epistatic to *Ve⁺*). Unfortunately, the dominant *Venosa⁺* (*Ve⁺*) accession, described by Stubbe (1966), has been lost from the Gatersleben germplasm collection. However, after outcrossing of another Gatersleben accession, *decipiens*, to stocks from the collection at the John Innes Centre, including *ros^{col}* and *ros^{dor}*, segregation of the *Ve⁺* phenotype was apparent. Wild type accessions (John Innes Centre stocks 7 and 522) carry the recessive *ve⁻* allele, as do the *ros^{dor}* and *ros^{col}* stock accessions. The *Ve⁺* allele in the *decipiens* accession is very closely linked to the recessive *decipiens* allele, and we have recovered no recombinants in examination of >300 F2 progeny. The *Ve⁺* phenotype segregates independently of *Rosea*; therefore, these two loci are unlinked.

Isolation of MYB-Related Genes Controlling Anthocyanin Biosynthesis from *A. majus*

To identify genes encoding MYB-related proteins controlling anthocyanin pigmentation in *A. majus*, oligonucleotide primers to the most conserved regions of MYB genes C1 (from maize) and AN2 (from *Petunia*), which are the regions encoding the recognition helices of the DNA binding domain (Figure 2A), were used for 3' rapid amplification of cDNA ends (RACE) PCR amplification of cDNA from flowers of the wild type and *rosea*, *Eluta*, and *mut* mutants. cDNA fragments were amplified from wild-type flowers with an oligonucleotide encoding part of the first recognition helix

RACE PCR amplification using oligonucleotide G1709 and the adaptor oligonucleotide (Frohmann et al., 1988) on first-strand cDNA from flowers of wild-type, *ros^{col}*, and *ros^{dor}* individuals. The arrow indicates the band present in the wild type and missing from *rosea* cDNAs.

(C) Maps of independent λ EMBL4 clones identified as containing the *Ros1* and/or *Ros2* genes.

(D) Map of the *Rosea* locus from wild-type *A. majus*. The raised blocks indicate exon sequence. The initiating ATG codons for *Ros1* and *Ros2* are shown. Restriction enzyme sites are as follows: E, *EcoRI*; X, *XbaI* (only relevant sites are shown). The 2.4-kb *XbaI* fragment mentioned in the text is also indicated.

(E) Map of the *Rosea* locus from *ros^{col}*. The raised blocks indicate exon sequence. The initiating ATG codons for *Ros1* and *Ros2* are shown. Changes from the wild-type sequence are indicated by red lines.

(F) Map of the *Rosea* locus from *ros^{dor}*. The raised blocks indicate exon sequence. The initiating ATG codon for *Ros1* is shown. Changes from the wild-type sequence are indicated by red lines.

and with one encoding part of the second recognition helix. One of the fragments amplified by the oligonucleotide from the first recognition helix in R2 (G1709) was not present when cDNA from flowers of *ros^{dor}* or *ros^{col}* were used (Figure 2B). This fragment was amplified from cDNA from flowers of the other mutants.

The cDNA fragment amplified by 3' RACE from wild-type flower buds using the G1709 oligonucleotide as a primer was used to probe a cDNA library made from wild-type flowers of *A. majus*. Two cDNA clones (that hybridized under high-stringency washing conditions) were identified. These were subcloned into pBluescript SK+ and sequenced. Both cDNA clones contained the same open reading frame (ORF) but contained slightly different lengths of 5' and 3' untranslated region. Both contained the complete ORF encoding a MYB-related protein very similar to AN2. This gene product was named *Rosea1* (*Ros1*) (see Supplemental Figure 1 online).

Genomic clones encoding the *Ros1* gene were isolated by screening a genomic library from *A. majus* in λ EMBL4 (a gift from Hans Sommer) with the *Ros1* cDNA. Five positive clones were identified and mapped (Figure 2C). Two of the independent genomic clones contained the *Ros1* coding sequence within three adjacent *EcoRI* fragments. They also contained a second region of homology with the *Ros1* cDNA, situated 4.3 kb downstream of *Ros1* within a 2.4-kb *XbaI* fragment (Figure 2D). The three other clones contained only the second region of homology defined by the 2.4-kb *XbaI* fragment (Figures 2C and 2D). The sequences of the three *EcoRI* fragments containing the genomic sequence for *Ros1* were determined. The ORF was interrupted by two introns situated at equivalent positions to the introns in the *C1* gene of maize (Paz-Ares et al., 1987) and *AN2* from *Petunia* (Quattrocchio et al., 1999), the first of 231 bp and the second of 1498 bp (Figure 2D). There was a sequence, TATTT, located 115 bp upstream of the initiating ATG in *Ros1* that approximates a plant TATA binding site (Molina and Grotewold, 2005). Farther upstream at -489 and -587 were two additional motifs (TATAA) that approximated better to the TATA binding consensus.

The second region of homology with the *Ros1* cDNA (contained within the 2.4-kb *XbaI* fragment) in all five λ EMBL4 clones was also sequenced (Figure 2C). This contained a sequence encoding the N-terminal region of a second MYB-related protein, distinct but structurally very similar to the N terminus of *Ros1*. This gene fragment was termed *Rosea2* (*Ros2*). All five λ clones ended within the second intron of *Ros2*, and we were unable to identify any overlapping clones that contained the downstream ORF of *Ros2*. To determine whether this second gene was expressed and functional, we examined the expression of *Ros2* in the wild type and *ros* mutant lines.

The *Ros2* cDNA was amplified by 3' RACE PCR (Frohmann et al., 1988) using an oligonucleotide primer to the sequence encoding the initiating ATG codon of the *Ros2* protein in the genomic clone and cDNA made from flowers of *ros^{col}*. A cDNA fragment was amplified that contained the entire *Ros2* ORF, 3' to the priming oligonucleotide (Figure 3B). Comparison with the partial genomic sequence of *Ros2* confirmed that it contained at least two introns, the first two being in identical positions to those in *Ros1*, *An2* from *Petunia*, and *C1* and *Pl* from maize. The first intron in *Ros2* was 111 bp, whereas the size of the second intron remains unknown but it is >9 kb, as deduced from the genomic

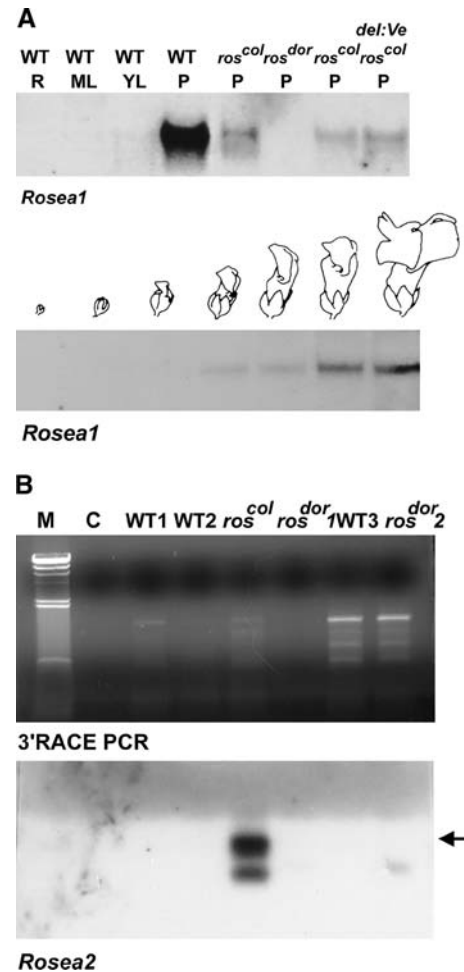


Figure 3. Expression of *Rosea* Genes in Flowers of Wild-Type *A. majus* and *rosea* Mutants.

(A) RNA gel blot of poly(A)⁺ RNA from different organs of wild-type *A. majus* (R, root; ML, mature leaf; YL, young leaf; P, petal) and from petals of *ros^{col}*, *ros^{dor}*, and *ros^{col} Ve⁺* lines probed with the *Ros1* cDNA. Below, the expression of *Ros1* is shown at different stages of petal development. Maximum expression was observed when the flowers had just opened.

(B) Ethidium bromide-stained agarose gel of 3' RACE PCR products produced using oligonucleotide K17 and the adaptor oligonucleotide (Frohmann et al., 1988) on first-strand cDNA from flowers of wild-type, *ros^{col}*, and *ros^{dor}* individuals. Below is a blot of the same gel probed with a fragment of the *Ros2* gene. The arrow indicates cDNA that was amplified from *ros^{col}* only. M, size markers of λ DNA digested with *HindIII*; C, control amplification without cDNA.

sequences in the λ EMBL4 clones available. A potential TATA box was identified 109 bp upstream of the first ATG in the *Ros2* ORF (Figure 2D).

Further analysis of the 3' end of the *Ros2* gene in the wild type, *ros^{col}*, and *ros^{dor}* by PCR amplification using primers from the cDNA clone revealed that the sequences lying 3' to the second intron in *Ros2* were present in the genomes of both wild-type and *ros^{col}* lines. There were eight single-nucleotide differences in this

region between these two lines (Figure 2E), one of which caused a change in the encoded amino acid sequence (Lys-124 to Iso-124; Ros2 numbering). In *ros^{dor}*, the equivalent region was highly rearranged; the sequence encoding the recognition helix of R3 of Ros2 was missing in the *ros^{dor}* line (Figure 2F). The sequences farther downstream were present but rearranged, including six single-nucleotide differences between *ros^{dor}* and *ros^{col}* and the insertion of a transposon that interrupted the Ros2 ORF at codon 206 (Glu-206). The transposon had 11-bp terminal inverted repeats and had generated a 9-bp direct duplication in the Ros2 ORF upon insertion.

Genotypic Constitution of Wild-Type, *ros^{col}*, and *ros^{dor}* Lines at the *Rosea* Locus

Because *Ros1* cDNA was not amplified using the G1709 oligonucleotide primer from cDNA derived from RNA from flowers of either *ros^{dor}* or *ros^{col}*, the possibility that the phenotypes conferred by *rosea* resulted from mutations in the *Ros1* or *Ros2* gene was investigated at the molecular level. First, the linkage of the two genes to the *ros* mutations was analyzed in crosses between the wild type and *ros^{col}* and the wild type and *ros^{dor}*. The *Ros1* gene was highly polymorphic between wild-type, *ros^{col}*, and *ros^{dor}* lines. Using *EcoRI* digests, 126 progeny were examined from F2 crosses between the wild type and *ros^{col}* and 96 progeny were examined from crosses between the wild type and *ros^{dor}*. The *ros^{col}* and *ros^{dor}* plants that segregated (scored phenotypically) in F2 were all homozygous for the parental versions of the *Ros* locus identified in the stock *ros^{col}* and *ros^{dor}* lines.

The expression of *Ros1* in the wild type, *ros^{col}*, and *ros^{dor}* was examined by RNA gel blot analysis. A high level of transcript was detected in maturing petals of wild-type plants (Figure 3A). A considerably reduced level of transcript of a slightly smaller size accumulated in petals of the same age from *ros^{col}* (Figure 3A). This transcript was amplified by RT-PCR and sequenced. It contained several single-nucleotide substitutions compared with wild-type *Ros1*, but the most significant difference was a 64-bp deletion that included the region encoding the first recognition helix (in R2) of the DNA binding domain (Figure 2E). This mutation introduced a stop codon 36 bp downstream of the deletion, indicating that a nonfunctional *Ros1* product was produced, because the encoded protein would lack more than half of its DNA binding domain and the entirety of its C terminus. The 64-bp deletion included sequence encoding the recognition helix of R2, which explains why the original oligonucleotide, G1709, failed to amplify a cDNA product from *ros^{col}* RNA by 3' RACE PCR.

The *ros^{dor}* line produced no *Ros1* transcript detectable on RNA gel blots (Figure 3A). However, RT-PCR did amplify a *Ros1* cDNA that was cloned and sequenced. This showed 11 differences from the sequence of *Ros1* from wild-type lines, of which 8 affected the identity of the encoded amino acids (codon Glu-27 to Lys, Gly-116 to Arg, Leu-131 to Gln, Lys-174 to Thr, Thr-176 to Lys, Ala-183 to Val, Glu-190 to Asp, and Asp-191 to Glu). However, comparison with the sequences of Ros2 and Ve suggested that it was unlikely that any of these changes would contribute to the phenotype, implying that the primary change in *ros^{dor}* is a change in the expression pattern of *Ros1*. To check this, we cloned the genomic DNA encoding the promoter and

N terminus (up to the second intron) of *Ros1* from the *ros^{dor}* background. Within the 910-bp region of the *Ros1* promoter (compared between the wild type and *ros^{dor}*), there were nine single-nucleotide substitutions, two single-nucleotide additions, one single-nucleotide loss, and an insertion of 12 bp at 440 bp upstream of the initiating ATG codon. The biggest difference, however, was a deletion of 187 bp in the promoter (from -140 to -326), which is likely to have a significant impact on the transcription of *Ros1*.

The expression of the full-length *Ros2* transcript was analyzed using RT-PCR. Using a 5' oligonucleotide covering the initiating ATG of *Ros2* and a reverse primer representing sequences in the 3' untranslated region, a full-length transcript was detected in *ros^{col}* flowers but not in wild-type or *ros^{dor}* flowers (Figure 3B). These data showed that *ros^{col}* expresses a full-length transcript of *Ros2* at a very low level, but there is no expression of full-length *Ros2* in the wild type or *ros^{dor}*. Therefore, the wild type and *ros^{dor}* were deemed to be *ros2⁻*.

These data suggested that both *ros^{col}* and *ros^{dor}* are determined by mutations in the complex *Rosea* locus. *ros^{col}* carries a loss-of-function allele of *Ros1* but expresses *Ros2*. The *Ros2* gene contributes the weak pigmentation restricted to the inner epidermis of the corolla lobes and the base of the tube seen in *ros^{col}*, but it is not expressed in wild-type lines. *ros^{dor}* has no *Ros2* expression and so no pigment on the inner epidermis of the lobes. *Ros1* expression is modified in *ros^{dor}*, most likely as a result of changes to the promoter of *Ros1*, such that it induces pigmentation only in the outer epidermis of the dorsal petals and in a ring at the base of the tube under specific environmental conditions of high light and relatively low temperature. Its contribution to vegetative pigmentation compared with the wild type is relatively normal.

To confirm that *Ros1* and *Ros2* both control anthocyanin production, and that *Ros1* and *Ros2* could complement *rosea* mutants, we used particle bombardment of *ros^{dor}* lines grown in the greenhouse, so that the corolla lobes were acyanic. Each cDNA was cloned between the cauliflower mosaic virus (CaMV) 35S promoter and the octopine synthase terminator and was bombarded into the inner epidermis of the dorsal petals of *ros^{dor}* flowers, as well as a control plasmid containing β -glucuronidase (GUS) driven by the 35S promoter. In tissue bombarded with the control plasmid alone, patches of gold were visible after 2 d (Figure 4A). The gold particles were surrounded by tissue that had browned slightly as a result of physical damage from bombardment. No spots of magenta anthocyanin pigment were ever observed with the control plasmid (Figure 4A). However, histochemical GUS staining revealed that the control plasmid was active in the bombarded tissue (Figure 4B). Bombardment with the *Ros1* cDNA resulted in the development of single magenta cells within 48 h of bombardment. On average, for *Ros1* >100 spots were observed per replicate piece of petal (Figures 4C and 4D). Bombardment with *Ros2* also gave rise to magenta spots, but at a lower frequency than in *Ros1* (Figure 4D).

These experiments showed that the *Rosea* locus is complex, consisting of two very closely linked genes, *Ros1* and *Ros2*. Loss of function of *Ros1* gives rise to the *ros^{col}* phenotype, whereas modified and severely reduced expression of *Ros1* and loss of function of *Ros2* gives rise to the *ros^{dor}* phenotype.

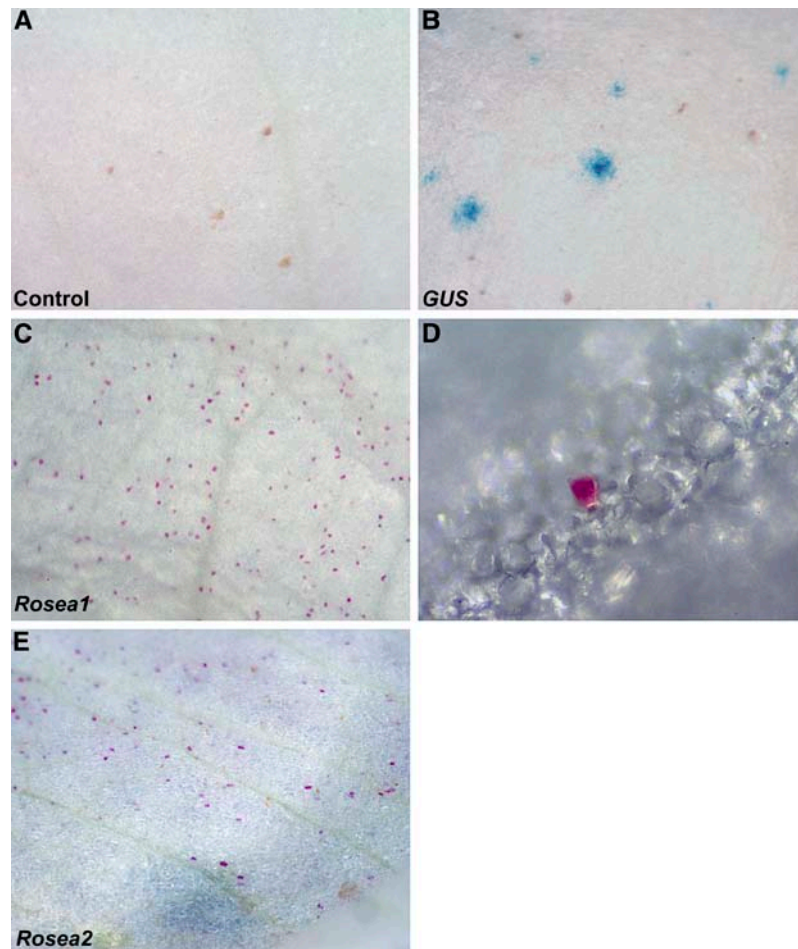


Figure 4. Complementation of the Mutant Phenotype Conferred by *ros^{dor}* by Particle Bombardment of Petal Lobe Tissue with the *Rosea* Genes.

- (A) Petal tissue bombarded with a construct carrying the *GUS* gene under the control of the CaMV 35S promoter. Only patches of gold are visible.
 (B) Tissue bombarded with a construct carrying the *GUS* gene under the control of the CaMV 35S promoter, stained for *GUS* activity.
 (C) Petal tissue bombarded with a construct with the *Ros1* gene expressed under the control of the 35S promoter.
 (D) Magnification of tissue shown in (C), demonstrating magenta anthocyanin being produced in single petal epidermal cells.
 (E) Petal tissue bombarded with a construct with the *Ros2* gene expressed under the control of the 35S promoter.

A Third Unlinked Gene Encoding a MYB-Related Protein Controls the Phenotype Conferred by *Venosa*

Because the *Ve⁺* allele confers strong magenta pigmentation to the epidermal cells overlying the petal veins in *ros* mutants, but other structural and regulatory mutations are epistatic to *Ve⁺*, we reasoned that *Venosa* most likely encodes a MYB-related transcription factor that was functionally similar to *Ros1* and *Ros2*. To identify such a gene, we digested genomic DNA from *Ve⁺/ve⁻* heterozygotes and *ve⁻* homozygotes with a range of restriction enzymes, separated the DNA by gel electrophoresis, and blotted it onto nitrocellulose filters. The DNA gel blots were probed with a fragment of cDNA encoding the *Ros1* MYB DNA binding domain and were subsequently washed at low stringency. The *EcoRI* digest revealed a number of hybridizing bands, one of which (2.9 kb) segregated clearly with the phenotype conferred by *Ve⁺* (Figure 5A). This fragment of genomic DNA was cloned from DNA

from a *Ve⁺/ve⁻* heterozygote in λ NM1149 and subsequently was subcloned in pBluescript SK+ and sequenced. The genomic DNA fragment contained the sequence encoding the N-terminal region of a MYB-related transcription factor. This sequence was used to design a gene-specific primer to the sequence, including the initiating ATG. This oligonucleotide was used for 3' RACE PCR on cDNA prepared from *Ve⁺* and *ve⁻* corolla tissue. A transcript was amplified only from *Ve⁺* cDNA. This was cloned and sequenced. The *Ve* cDNA encoded an R2R3 MYB protein very similar to *Ros1* and *Ros2* (see Supplemental Figure 1 online). By comparison with the genomic DNA of the active allele, the gene was deduced to have at least two introns, the first of 480 bp and the second of 1450 bp. The 5' upstream region contained a motif, TATAT, 75 bp upstream of the initiating ATG, and another, TTATTT, 101 bp upstream. Either of these may constitute the TATA box. The cDNA clone was used to map the *Ve* gene relative to the phenotype conferred by *Ve⁺* in 179 segregating F2 individuals.

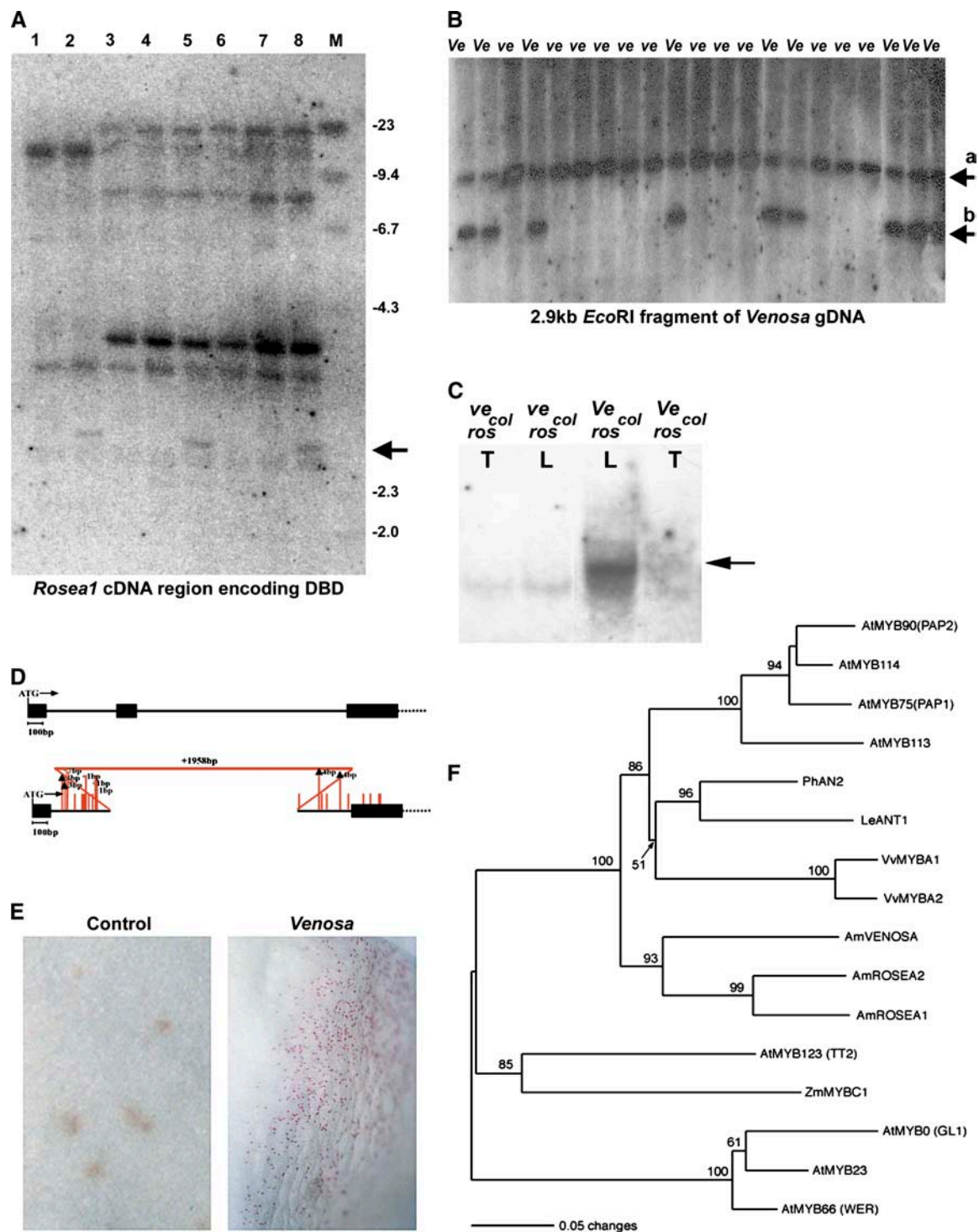


Figure 5. Identification of the *Venosa* Gene and Phylogenetic Analysis of the MYB Proteins Encoded by *Ros1*, *Ros2*, and *Ve*.

(A) DNA gel blot of genomic DNA from individuals with different *Ve* phenotypes digested with *Eco*RI and probed with the region of the *Ros1* cDNA encoding the DNA binding domain. Washing was at low stringency. The arrow indicates a fragment of DNA present only in lines carrying the *Ve*⁺ allele. Lane 1, *ros*^{dor}; lane 2, *ros*^{dor} *Ve*⁺; lanes 3, 4, 6, and 7, *ros*^{col}; lanes 5 and 8, *ros*^{col} *Ve*⁺.

(B) Mapping of the 2.9-kb *Eco*RI fragment identified in (A). Genomic DNA from individuals with the phenotype indicated above the line was digested with *Eco*RI and probed with the 2.9-kb *Eco*RI fragment from the *Venosa* locus. Arrow a indicates a *ve*⁻ allele, and arrow b indicates a *Ve*⁺ allele.

No recombinants were found between the phenotype conferred by Ve^+ and the 2.9-kb *EcoRI* fragment (Figure 5B).

RNA from flowers of *ros* lines with or without the Ve^+ phenotype was examined for the expression of *Ve* by RNA gel blot analysis (Figure 5C). *Ve* transcript was detected in the lobes and to a lesser extent in the tubes of Ve^+ lines, but no transcript was detected in ve^- lines, confirming the 3' RACE results. Genomic DNA encoding the *Ve* gene from the ve^- allele was also cloned from the Ve^+/ve^- heterozygote. The ve^- allele had several differences in sequence from the functional Ve^+ allele, most significantly the replacement of a 1221-bp region of the gene from the middle of the first intron to the middle of the second intron with an unrelated sequence of 1958 bp (Figure 5D). This removed the second exon of the gene, a change likely to render the protein nonfunctional. The 1958-bp insertion sequence showed no significant similarity to sequences of known function on a search of the GenBank databases. However, it did include direct flanking repeats of 40 bp, suggestive of the sequence of a transposon. Other differences in sequence between the Ve^+ and ve^- alleles were minor, consisting of 23 mostly single-nucleotide changes over the 3158-bp sequence of *Ve* analyzed (Figure 5D). None of these resulted in changes to the encoded amino acid residues.

To confirm that *Ve* could regulate anthocyanin biosynthetic gene expression, the cDNA was cloned between the double CaMV 35S promoter and the octopine synthase terminator and was bombarded into *ros^{dor}* petals (greenhouse-grown). A large number (>100 per replicate) of magenta single-cell spots were observed within 48 h, whereas the control plasmid gave no magenta spots (Figure 5E).

Ve*, *Ros1*, and *Ros2* Appear to Have Arisen by Gene Duplication in *Antirrhinum

The deduced amino acid sequences of the *Ros1*, *Ros2*, and *Ve* peptides were compared with those of other MYB proteins identified as regulators of flavonoid biosynthesis: AN2 from *Petunia* (Quattrocchio et al., 1999), Vv MYBA1 and Vv MYBA2 from grape (*Vitis vinifera*) (Kobayashi et al., 2002), TT2 (At MYB123), PAP1 (At MYB75), PAP2 (At MYB90), At MYB113, and At MYB114 from *Arabidopsis*, and C1 and PI from maize. GLABROUS1 (GL1), WERWOLF (WER), and At MYB23 from *Arabidopsis* (Stracke et al., 2001) were included as outgroups (Figure 5F; see Supplemental Figure 1 online). All of the anthocyanin-regulatory MYB proteins were very similar over their DNA binding domains, with 59 of 100 amino acids in the R2R3 MYB DNA binding domain conserved in all proteins. In R2R3 MYBs, the DNA binding domain forms two

repeats of helix-helix-turn-helix structure. The third helix in each repeat is believed to interact with DNA to bind it in a sequence-specific manner. The greatest conservation of sequence between these proteins was in the third region of α helix in R2 and in the second region of α helix in R3 (see Supplemental Figure 1A online). Surprisingly, there were quite a number of amino acid substitutions within the third helix (the recognition helix) of R3 between *Ros1*, *Ros2*, and *Ve*, suggesting that the different proteins might have somewhat different binding site preferences (see Supplemental Figure 1 online).

Several amino acids within helix 1 and helix 2 of R3 have been identified by Grotewold et al. (2000) as important for interaction with bHLH proteins (Leu-76, Arg-79, Arg-82, Leu-83, Gly-94, and Arg-95; C1 numbering). All are conserved in *Ros1*, *Ros2*, and *Ve*. The extended interaction signature identified by Zimmermann et al. (2004) as [DE]Lx₂[RK]x₃Lx₆Lx₃R is also conserved and identical in the R3 regions of *Ros1*, *Ros2*, and *Ve* (DLivRIhKLignkwsLiagR; where uppercase letters indicate amino acids that are completely conserved, lowercase letters indicate alternative amino acids, and x indicates any amino acid). This implies that all three *Antirrhinum* proteins interact with bHLH proteins in their activation of anthocyanin biosynthesis, as has been shown for C1, PI, and AN2.

The C-terminal domains of the *Antirrhinum* MYB regulators were much less well conserved, but one patch of conserved sequence was obvious: a more acidic region toward the C terminus of each protein that surrounds a core sequence of higher conservation (in dicot MYB proteins, it was Ww/lx+/-LL, where the annotation is as before and +/- indicates a charged amino acid). This motif is part of a longer motif identified by Kranz et al. (1998) from *Arabidopsis* MYB proteins defining R2R3 MYB subgroup 6. This short motif shows similarity to sequence in the KIX domain of animal c-MYB, which lies within the activation domain of that protein and interacts with the transcriptional coactivator, CREB. In C1 and PI, there are also acidic regions at the C termini of the proteins structured around the sequence WLRC+T, which might represent the equivalent domain in the monocot proteins. One residue, Asn, which lies immediately N terminal to the WLRC+T motif, has been shown to contribute significantly to the ability of the C-terminal domain of C1 to activate transcription (Sainz et al., 1997a). The C-terminal domains of C1 and AN2 have also been shown to activate transcription in yeast one-hybrid assays (Goff et al., 1992; Sainz et al., 1997a; Quattrocchio et al., 1999).

Phylogenetic analysis of the anthocyanin MYB regulators *Ros1*, *Ros2*, and *Ve* was performed. A well-supported phylogeny was recovered that placed the *Antirrhinum* proteins as more

Figure 5. (continued).

- (C) RNA gel blot of poly(A)⁺ RNA from petal tissue of *ros^{col} Ve⁺* and *ros^{col} ve⁻* lines probed with the *Ve* cDNA. The arrow indicates the *Ve* transcript. L, lobes; T, tubes of flowers.
- (D) Top, map of the *Ve* locus from wild-type *A. majus*. The raised blocks indicate exon sequence. The initiating ATG codon is shown. Bottom, map of the *Ve* locus from *ve⁻*. Differences from the wild-type sequence are indicated by red lines.
- (E) Left, petal tissue bombarded with an empty vector construct; right, petal tissue bombarded with a construct with the *Venosa* gene expressed under the control of the 35S promoter.
- (F) Phylogenetic tree comparing the amino acid sequences of the DNA binding domains of the R2R3 MYB subgroup 6 members. The regions used for the alignments are indicated in Supplemental Figure 1 online. The numbers indicate bootstrap values.

closely related to one another than to their orthologs from other species (Figure 5F; see Supplemental Figure 1 online). This suggested that the three *Antirrhinum* genes were derived from relatively recent duplications of a common ancestral gene. The first duplication created the unlinked genes, the progenitor of *Venosa* and the progenitor of *Rosea*. The second duplication gave rise to *Rosea1* and *Rosea2* and occurred intrachromosomally. Similar duplication events appear to have also occurred recently in *Arabidopsis* to create *MYB75*, *MYB90*, *MYB113*, and *MYB114*, which are clustered on chromosome 1 (Stracke et al., 2001), in grape to create *MYBA1* and *MYBA2*, which are closely linked (Kobayashi et al., 2002, 2004, 2005), in tomato (*Lycopersicon esculentum*) to create *ANT1* and a very closely linked MYB-like gene (Mathews et al., 2003; De Jong et al., 2004), and in potato (*Solanum tuberosum*) to create the linked *F* locus controlling floral pigmentation and the *D(l)* locus controlling tuber color (De Jong et al., 2004); a duplication of the whole genome may have created *C1* and *Pl* in maize (Cone et al., 1993).

Comparison of the Effects of Ros1, Ros2, and Ve on Target Gene Expression Reveals the Proteins to Have Similar but Distinct Biochemical Specificities

Although Ros1, Ros2, and Ve can all activate anthocyanin biosynthesis, we were interested to know whether they are truly functionally identical proteins or whether they have evolved distinct specificities in their regulatory properties. To this end, we examined the target genes of Ros1, Ros2, and Ve by comparing the levels of transcripts encoding the enzymes of anthocyanin biosynthesis in plants, both wild type and mutant, for the expression of each regulatory gene. To analyze the effects of Ros1, we compared the expression of the biosynthetic genes in flowers of the wild type and *ros^{dor}* (Figure 6). No change in transcript levels was observed for *CHS*. A small decrease in the level of chalcone isomerase (*CHI*) transcript was observed in *ros^{dor}* petals compared with wild-type petals. Much less transcript was observed in *ros^{dor}* than in the wild type for *F3H*, although greater differences were observed for *F3'H*, *DFR*, and *UFGT*. Smaller but still significant reductions in transcript levels in *ros^{dor}* compared with the wild type were observed for flavonol synthase (*FLS*), *ANS*, and *AT*, an anthocyanin permease from *A. majus* (GenBank accession number AJ796511) homologous with a tomato MATE transporter induced by a MYB transcription factor regulating anthocyanin production in tomato (Mathews et al., 2003; Bey et al., 2004). These data showed that Ros1 increases the transcript levels of the late biosynthetic genes (*F3H*, *DFR*, *ANS*, and *UFGT*) as well as *F3'H*, *FLS*, and *AT*, although not all of these target genes are equally dependent on Ros1 activity. *F3'H*, *F3H*, *DFR*, and *UFGT* were particularly dependent on Ros1 activity, because virtually no transcripts for these genes were detected in *ros^{dor}* flowers. By contrast, *ANS* and *AT* were much less dependent on Ros1. Ros1 was not required for the accumulation of transcripts of the early biosynthetic gene *CHS* and had only a very minor influence on *CHI*. This is similar to the effect of Delila on the regulation of the anthocyanin biosynthetic pathway in *Antirrhinum* (Martin et al., 1991), supporting the view that Ros1 may interact with Delila to activate gene transcription.

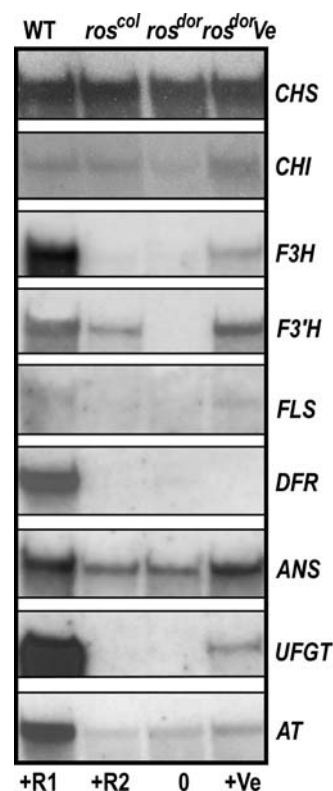


Figure 6. RNA Gel Blots of Poly(A)⁺ RNA from Petal Tissue of Wild-Type, *ros^{col}*, *ros^{dor}*, and *ros^{dor} Ve⁺* Plants Probed with cDNA Fragments of the Genes Encoding the Enzymes of the Anthocyanin Biosynthesis Pathway.

The composition of active MYB proteins in each genotype is shown below the blots. R1, *Rosea1*; R2, *Rosea2*; Ve, *Venosa*. Genes assayed were as follows: *CHS*, gene encoding chalcone synthase; *CHI*, chalcone isomerase; *F3H*, flavanone 3-hydroxylase; *F3'H*, flavonoid 3'-hydroxylase; *FLS*, flavonol synthase; *DFR*, dihydroflavonol 4-reductase; *ANS*, anthocyanidin synthase; *UFGT*, UDP-glucose 3-O-flavonoid transferase; *AT*, anthocyanin transporter.

The influence of Ros2 on biosynthetic gene expression was assayed by comparing expression in *ros^{col}* with expression in *ros^{dor}* (Figure 6). *ros^{dor}* does not express *Ros2* and has virtually undetectable levels of expression of *Ros1* (Figure 3A). Consequently, comparison of expression of the biosynthetic genes in *ros^{col}* and *ros^{dor}* revealed the influence of Ros2 on biosynthetic gene transcript levels. No differences were observed in transcript levels of *CHS*. A small increase in transcript levels of *CHI* was observed in *ros^{col}* compared with *ros^{dor}*. However, significantly lower levels of *F3'H* transcripts were observed in *ros^{dor}* compared with *ros^{col}*, suggesting that Ros2 regulates the expression of *F3'H* and possibly, in contrast with Ros1, contributes to the activation of *CHI*.

The influence of Ve on anthocyanin biosynthetic gene expression was assayed by comparing transcript levels in *Ve⁺* and *ve⁻* lines in the *ros^{dor}* background (Figure 6). No difference was detected in the levels of *CHS* transcripts. The presence of an active *Ve⁺* allele did increase the transcript levels of *CHI*, *F3H*, *F3'H*, *FLS*, *ANS*, *UFGT*, and *AT*. Surprisingly, no difference could

be detected in the levels of *DFR* transcript between Ve^+ and ve^- lines; virtually no transcript was detected in either line. These data showed that *Ve* does increase the transcript levels of most of the biosynthetic genes and is not required for the expression of the early gene, *CHS*. However, they also indicate that *Ve* does not activate *DFR* expression nearly as effectively as *Ros1*. These data imply that there are subtle but reproducible differences in the abilities of *Ve*, *Ros1*, and *Ros2* to activate the transcription of different target genes. This could reflect differences in target site specificity affecting the affinity with which each activator binds to the target promoters of the different biosynthetic genes. Such specificity might also involve differences in the efficacy of the complexes that each MYB protein makes with the bHLH and WD repeat proteins.

Ros1 and Ve Show Differences from Ros2 in the Specificity of Their Interaction with the bHLH Regulator *Mut*

We examined the interactions of the different MYB transcription factors with bHLH proteins through genetic analyses. The *Delila* gene product is a bHLH protein that is required for anthocyanin biosynthesis in the corolla tubes. It is also expressed in the lobes, as demonstrated by in situ hybridization, and it is active in the lobes (Almeida et al., 1989; Goodrich et al., 1992). A second gene, *Mut*, is required for anthocyanin biosynthesis in the lobes if *Delila* is nonfunctional. This encodes another bHLH protein (P. Piazza, C. Tonelli, and C. Martin, unpublished data). The specificity of *Ros1*, *Ros2*, and *Ve* interactions with these two bHLH proteins was tested by making double and triple mutants.

The line mutant for *mut* and *del* is acyanic. Ve^+ is not visible in this background, suggesting that *Ros1*, *Ros2*, and *Ve* must interact with either *Del* or *Mut* to activate anthocyanin biosynthesis. When *ros^{dor}* is combined with *del*, the tubes are unpigmented, but there is little effect on pigmentation in the lobes, indicating that *Del* interacts with *Ros1* in the tubes but that in the lobes *Ros1* interacts with *Mut* to direct anthocyanin biosynthesis. This confirms the phenotype of *del* alone, in which the tubes are acyanic but the lobes (principally the product of *Ros1* and *Mut* interaction) have wild-type levels of pigmentation.

When *ros^{col}* (in which only *Ros2* of the MYB regulators is expressed) was combined with *del*, the double mutant was completely acyanic, despite *Ros2* being active in the lobes (cf. Figures 7A and 7B). This indicates that in the lobes, *Ros2* can interact with *Del* but not with *Mut*. This could be because *Ros1* activates the expression of *Mut*, because in *Petunia* the AN2 MYB protein has been reported to activate the expression of *AN1* (encoding a bHLH protein) in leaves (although not in flowers) (Spelt et al., 2000). However, although when *ros^{col}* *Ve* was combined with *del* the background pigmentation in the corolla lobes of these plants was missing (acyanic), the venal pattern, determined by *Ve*, remained distinct (cf. Figures 7C and 7D). These results indicated that although *Ros2* interacts effectively only with *Del* in the lobes, *Ve* (like *Ros1*) can interact effectively with *Mut*. These interactions are summarized in Figure 7E. Because our analysis of target gene activation showed that the three MYB proteins, *Ros1*, *Ros2*, and *Ve*, had differential specificities for each of the target genes, the ineffectual interaction between *Ros2* and *Mut* may reflect the loss of activity of these

proteins on a single target promoter, or their lack of activity on all target promoters. These possibilities cannot be resolved through genetic analysis, which measures only the accumulation of the end product, anthocyanin, and not the activation of the individual biosynthetic genes.

Variation in Anthocyanin Patterns in Flowers of Different *Antirrhinum* Species Results Principally from Variation in the Activity of the MYB-Related Genes

Many different species of *Antirrhinum* have been described, some native to North America and some native to Europe. On the European branch of the genus, whose members are diploid, *A. majus* is one of several species that have strong, self-colored anthocyanin pigmentation of the corolla, others being *Antirrhinum australe* and *Antirrhinum barrelieri* (Figures 8E and 8F). Other closely related species include *Antirrhinum latifolium*, *Antirrhinum graniticum*, *Antirrhinum molle*, *Antirrhinum mollissimum*, and *Antirrhinum meonanthemum*. These species vary in their floral pigmentation and typically all have a very pale or no background anthocyanin accumulation in their corolla lobes. The floral pigmentation phenotypes of accessions of these species are shown in Figure 8 and tabulated in Table 1. We analyzed two wild accessions of *A. majus* subsp. *majus* originating from Toulouse (Figures 8A and 8B) and Barcelona (Figures 8C and 8D), which both had medium-intensity anthocyanin accumulation in the corolla with a weak venal pattern superimposed. Two *A. latifolium* accessions had no background anthocyanin pigmentation but a clear venal pattern of accumulation (Figures 8G and 8H). In addition to the restricted anthocyanin pattern, both *A. latifolium* accessions showed strong aurone production all over their corolla lobes, giving them a pale yellow color typical of *A. latifolium* (Stubbe, 1966). Four other accessions were analyzed. These were *A. graniticum*, which had very weak anthocyanin accumulation in the inner epidermis of the corolla lobes but no evidence of venal patterning (Figure 8I); *A. molle*, which had no background pigmentation to the corolla lobes but a clear venal patterning of anthocyanin accumulation (Figure 8K); *A. mollissimum*, which had a weak background pigmentation and strong venal patterning in its floral pigmentation (Figure 8L); and *A. meonanthemum*, which had no background pigmentation to the corolla lobes but a clear venal patterning of anthocyanin accumulation and strong aurone production all over the corolla lobes, giving flowers a pale yellow color (Figure 8J) (Oyama and Baum, 2004). All of these accessions conformed to the general descriptions of floral pigmentation for the appropriate species (Sutton, 1988).

Despite strong self-incompatibility in some of these accessions (*A. graniticum*, *A. meonanthemum*, and *A. barrelieri*), all can cross-hybridize with *A. majus*. Therefore, we were able to test the genetic basis for the weak pigmentation in *A. graniticum*, *A. molle*, *A. mollissimum*, *A. meonanthemum*, and *A. latifolium* by crossing them to the different mutants of *A. majus*. Although crosses of either of the wild accessions of *A. majus* to *ros^{dor}* gave F1 progeny with fully pigmented flowers, none of the accessions of the other five species tested was able to complement the *rosea* mutants (neither *ros^{dor}* nor *ros^{col}*), indicating that, in all, the genetic basis for the low levels of anthocyanin was attributable to

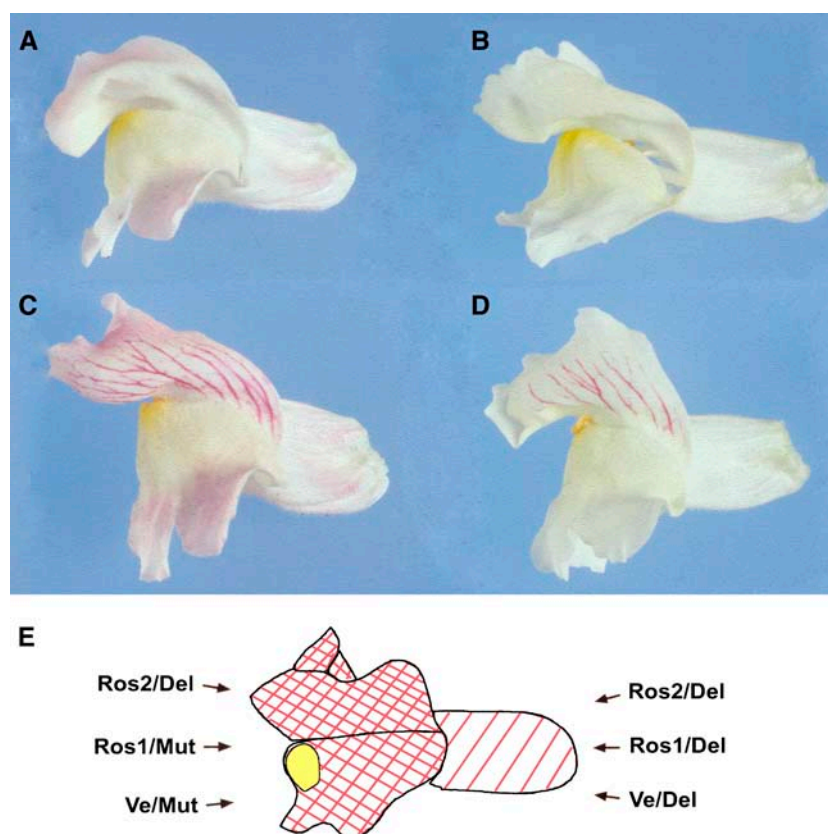


Figure 7. Interaction of MYB Proteins with bHLH Proteins Revealed by Mutant Analysis.

- (A) *ros^{col}*.
 (B) *ros^{col} del.*
 (C) *ros^{col} Ve⁺*.
 (D) *ros^{col} Ve⁺ del.*

(E) Diagram summarizing the interactions of the regulatory proteins in the different regions of the flower of *A. majus*. Red diagonal stripes sloping right indicate the area of *Mut* expression; red diagonal stripes sloping left indicate the area of *Del* expression. *Ros1* and *Ve* can interact with both *Mut* and *Del* in the lobes, whereas *Ros2* can interact only with *Del*.

the reduced activity of the *Rosea* locus compared with its activity in *A. majus*. Crosses of *A. graniticum*, *A. molle*, and *A. mollissimum* to wild-type *A. majus* gave rise to fully self-colored F1 progeny. In the F2 of these species crosses, the pale pigmentation phenotype segregated 1:3, indicating that variation at a single recessive locus was responsible for the pale pigmentation. The lack of complementation in these species crosses to the *ros^{dor}* line demonstrated this locus to be *Rosea*. Crosses of *A. graniticum*, *A. molle*, and *A. mollissimum* to *mut del* double mutants of *A. majus* gave rise to fully self-colored progeny, indicating that the activity of the *Mut* and *Del* genes does not limit pigmentation in these species (see Supplemental Figure 2A online).

Crosses of *A. meonanthemum* and *A. latifolium* to the *mut del* double mutant or to wild-type *A. majus* gave darker pigmentation to the lobes of flowers of the F1 progeny than that in *A. meonanthemum* and *A. latifolium*, but pigmentation was paler than in wild-type *A. majus*, especially over the outer edges of the corolla lobes (see Supplemental Figures 2B and 2C online). This phenotype matched exactly that of the *Eluta* mutant of *A. majus*

(Baur, 1910a; Stubbe, 1966) (Figures 1J to 1L), which is a semidominant diluter of anthocyanin pigment in flowers. In the F2 of these species crossed to wild-type *A. majus*, pale pigmentation, the diluted pigmentation phenotype, and full-red pigmentation segregated 1:2:1, respectively, indicating that the pale pigmentation in these species was attributable to a semidominant allele at a single locus. The fact that in F2 populations of *A. meonanthemum* and *A. latifolium* (Marseilles) crossed to *ros^{dor}*, no full-red plants segregated (30 and 96 progeny examined, respectively) indicated that both *A. meonanthemum* and *A. latifolium* carry semidominant alleles of the *Rosea* locus that dictate their pale floral pigmentation. These alleles are likely to be very similar in their activity to the *Eluta* mutant of *A. majus*. Indeed, *Eluta* has been reported to be very closely linked to *rosea* by Stubbe (1966). In F2 populations of *Eluta* crossed to *ros^{dor}* or *ros^{col}*, we have never observed full-red recombinants, supporting the idea that *Eluta* is a semidominant allele of the *Rosea* locus. We have indicated the semidominance of the pigment-diluting *Rosea* alleles in these species with the term *Ros^{El}*.

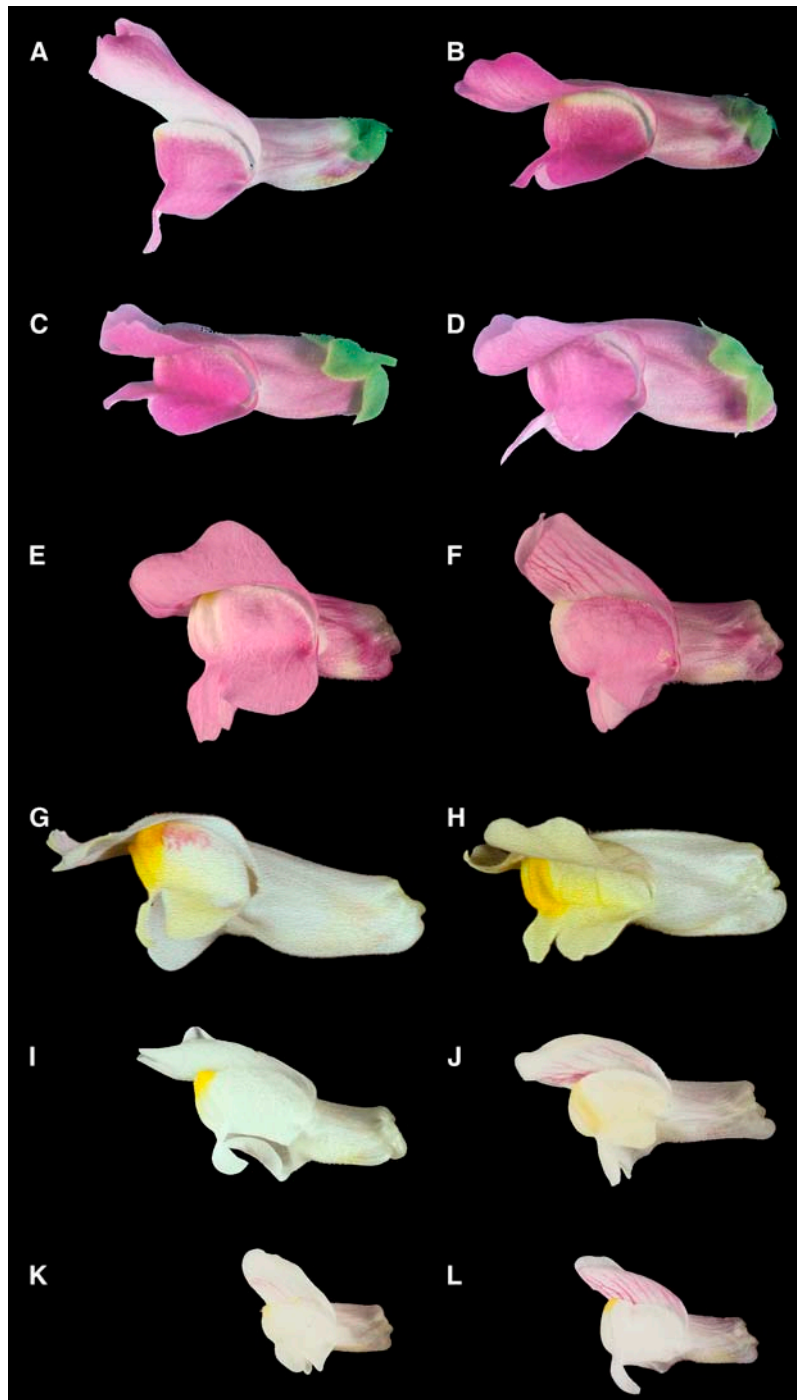


Figure 8. Floral Phenotypes of Accessions of Different Species within the Genus *Antirrhinum*.

- (A) *A. majus* subsp *majus* var *majus* (Toulouse) without venal pigmentation.
- (B) *A. majus* subsp *majus* var *majus* (Toulouse) with venal pigmentation.
- (C) *A. majus* subsp *majus* var *majus* (Barcelona) without venal pigmentation.
- (D) *A. majus* subsp *majus* var *majus* (Barcelona) with venal pigmentation.
- (E) *A. australe*.
- (F) *A. barrelieri*.
- (G) *A. latifolium* (Pyrea).
- (H) *A. latifolium* (Marseilles).

Table 1. Origins of Species Accessions, Floral Phenotypes, and Inferred Genotypes from Genetic Analysis

Species	Accession	Source	Floral Pigmentation Phenotype	Genotype
<i>A. majus</i>	Toulouse	IPK Gatersleben ^a	Medium-intensity magenta pigmentation, weak venal pattern (Figures 8A and 8B)	<i>Ros⁺/Ros⁺;Ve/ve</i>
	Barcelona	IPK Gatersleben	Medium-intensity magenta pigmentation, weak venal pattern (Figures 8C and 8D)	<i>Ros⁺/Ros⁺;Ve/ve</i>
<i>A. latifolium</i>	Pyrea	IPK Gatersleben	No background magenta pigmentation; venal pattern restricted to central part of dorsal lobes; yellow lobes (Figure 8G)	<i>Ros^{El}/Ros^{El};Ve/Ve;sulf/sulf</i>
	Marseilles	IPK Gatersleben	No background magenta pigmentation; venal pattern on dorsal lobes; yellow lobes (Figure 8H)	<i>Ros^{El}/Ros^{El};Ve/Ve;sulf/sulf</i>
<i>A. graniticum</i>	Spain	Harvard Herbarium	Very pale magenta pigmentation/no pigmentation (Figure 8I)	<i>ros/ros ve/ve</i>
<i>A. molle</i>	Spain	Harvard Herbarium	No background magenta pigmentation; strong venal pattern on dorsal lobes; yellowish lobes (Figure 8K)	<i>ros/ros;Ve/Ve;sulf/sulf</i>
<i>A. mollissimum</i>	Spain	Harvard Herbarium	No background magenta pigmentation; strong venal pattern on dorsal lobes (Figure 8L)	<i>ros/ros;Ve/Ve</i>
<i>A. meonantherum</i>	Spain	Harvard Herbarium	No background magenta pigmentation; strong venal pattern on dorsal lobes; yellow lobes (Figure 8J)	<i>Ros^{El}/Ros^{El};Ve/Ve;sulf/sulf</i>

^a IPK, Institut für Kulturpflanzenforschung.

Crosses of the species accessions to *ros^{dor}* suggested that *A. majus* subsp *majus* from both Barcelona and Toulouse was polymorphic for an active *Ve⁺* allele (Figures 8A to 8D). Crosses between these accessions and *ros^{dor} Ve* revealed that the venal patterning of pigmentation could be attributed to the activity of the *Ve* locus, because no unpatterned progeny segregated in the F2 population (see Supplemental Table 1 online). Similar analyses with the species showed that all *A. molle*, *A. mollissimum*, *A. meonantherum*, and *A. latifolium* individuals were homozygous for active *Ve⁺* alleles. The deduced genotypes of the species analyzed for the loci affecting floral pigmentation are listed in Table 1.

These data revealed that the loci controlling anthocyanin pigmentation patterning in different *Antirrhinum* species principally encoded MYB-related transcription factors. DNA gel blots revealed that all three genes, *Ros1*, *Ros2*, and *Ve*, are present in the genomes of each of the accessions tested. The differences in background pigmentation patterns between the different species (most readily observed in the F2 segregants from crosses to wild-type *A. majus*, in which genetic background is homogenized, allowing for easier comparisons) suggest that differences in the activity of the *Rosea* locus is the single most important determinant of pigmentation intensity in the species tested. In addition, the other MYB-related gene, *Venosa*, contributes significantly to pigmentation in *A. latifolium*, *A. molle*, *A. meonantherum*, and *A. mollissimum* and is also significant and variable in wild accessions of *A. majus* (see Supplemental Table 1 online).

DISCUSSION

In *Antirrhinum majus*, a small family of MYB-related proteins controls the pattern and intensity of floral pigmentation. Members of this family are closely related structurally to MYB proteins known to regulate anthocyanin production in other plant species, including maize (Paz-Ares et al., 1987; Cone et al., 1993) *Petunia* (Quattrocchio et al., 1999), grape (Kobayashi et al., 2002, 2004, 2005), pepper (*Capsicum annuum*) (Borovsky et al., 2004), morning glory (Chang et al., 2005), tomato (Mathews et al., 2003; De Jong et al., 2004), potato (De Jong et al., 2004), and *Arabidopsis* (Borevitz et al., 2000). Like other species, these different genes appear to have been derived by gene duplication and subfunctionalization, although our data from the investigation of mutant alleles suggests that the *Ros1*, *Ros2*, and *Ve* proteins are not functionally equivalent. These analyses were complicated by the different expression levels and patterns of the *Ros1*, *Ros2*, and *Ve* genes, but analysis of the transcript levels of potential target genes in lines defective in *Ros1*, *Ros2*, and *Ve* activity showed *F3H*, *F3'H*, *FLS*, *DFR*, and *UFGT* to be highly dependent on *Ros1* for induction, whereas *ANS* and *AT* were less dependent and *CHI* was very much less dependent on *Ros1* for induction. The only gene that was significantly induced by *Ros2* was *F3'H*, although *CHI* transcript levels were also increased to a small extent by this protein. *Ve* induced the expression of *CHI*, *F3H*, *F3'H*, *FLS*, *ANS*, *UFGT*, and *AT*, but its induction of *F3H*, *F3'H*, and *UFGT* was stronger than that for *ANS*.

Figure 8. (continued).

- (I) *A. graniticum*.
- (J) *A. meonantherum*.
- (K) *A. molle*.
- (L) *A. mollissimum*.

and *AT* and much stronger than that for *CHI*. Remarkably, *Ve* did not detectably activate *DFR* expression/transcript levels. These data suggest that each of these MYB proteins has distinct biochemical specificity in terms of its ability to activate transcription from different target promoters. This might reflect differences in their DNA binding affinities. There are a number of amino acid differences in the recognition helices of these three MYB proteins that could influence their DNA binding affinities and sequence motif recognition (see Supplemental Figure 1 online). Alternatively, differences in specificity might be attributable to differences in target promoter architecture, which could make binding or activation easier by one MYB protein relative to another, or to differences in the ability of the MYB regulators to interact with target promoters with different chromatin structures. However, although understanding of this specificity must await comparative biochemical characterization of the MYB proteins, we conclude that these regulatory proteins have diverged functionally as well as in their expression patterns, unlike the situation in maize, in which *C1* and *Pl* appear to be functionally equivalent (Cone et al., 1993).

Given the observed specificity for target gene activation by the three MYB proteins, it was surprising that all could complement the *ros^{dor}* mutation and produce pigmented cells after particle bombardment of petals (Figures 4C, 4E, and 5D). In addition, *Ve* can complement the loss of *Ros1* activity in the *ros^{col}* line to give regions of highly pigmented epidermal tissue (Figure 7C), and it can complement the loss of both *Ros1* and *Ros2* activity in *ros^{dor}* to give highly pigmented epidermal tissue in the regions overlying the veins on the inner epidermis of the petal lobes (Figure 1G). An explanation for this is that our complementation assays are based on the ability of cells to synthesize anthocyanins, an ability that is determined principally by the degree of activation of the biosynthetic step limiting the flux to anthocyanin accumulation in flowers. Although *DFR* was not detectably induced by *Ve* on RNA gel blots, 40 cycles of RT-PCR amplification of cDNA revealed low levels of *DFR* transcript in both *ros^{dor}* and *ros^{col}* flowers (see Supplemental Figure 3 online). This may be enough to allow anthocyanin biosynthesis if other steps, rate-limiting during flower development, are also induced. All of the data available for *Antirrhinum* flowers suggest that *F3H* catalyzes the step with greatest influence on the accumulation of anthocyanins (Martin et al., 1991). Consequently, the differing abilities of the MYB proteins to induce anthocyanin biosynthesis in *Antirrhinum* flowers are probably tied most closely to their relative abilities to induce *F3H* gene expression.

ros^{col} is a loss-of-function mutant of *Ros1* but expresses *Ros2*, although the latter gene is not expressed in wild-type *A. majus*. The basis for the absence of expression of *Ros2* in the wild type was not absolutely clear from molecular analysis, but it is probably related to the exceptionally large second intron in this gene. *Ros2* is expressed at very low levels in *ros^{col}* flowers: transcript could only be detected by PCR amplification. The low steady state levels of *Ros2* transcript in *ros^{col}* lines may be associated with inefficiency in splicing this large intron (which is of unknown size but is >9 kb), which is unusually large for plant genes. In wild-type *A. majus* lines, problems associated with the efficiency of splicing of the *Ros2* primary transcript (e.g., increases in intron size) might have escaped detection in our

analyses but could result in the abolition of mature *Ros2* transcript production.

In *ros^{dor}*, the *Ros2* gene is undoubtedly nonfunctional as a result of point mutations, deletions, and insertion of a transposon sequence within the ORF. In *ros^{dor}*, the promoter region of *Ros1* is highly modified compared with that in the wild type, suggesting significant differences in the control of expression of *Ros1* in the mutant line. This was confirmed by RNA gel blot and RT-PCR analyses. Both *ros^{col}* and *ros^{dor}*, therefore, show multiple sequence differences in both *Ros* genes compared with wild-type *A. majus*, and it is difficult to consider them as simple mutations (Figures 2D to 2F). Lines homozygous for either allele were identified very early in the history of plant genetics, being described by Baur (1910) in his original article on the genetics of floral pigmentation in *A. majus*. At that time, chemical mutagens were not in use, and it is likely that mutants were selected initially as natural variants. Given the ability of different *Antirrhinum* species to form fertile hybrids with *A. majus*, it seems quite likely that these *rosea* mutants were identified in natural populations and may have resulted from introgressions of the *Rosea* locus from other species. This idea is supported by phylogenetic analysis of the sequence of the third intron of the gene encoding nitrate reductase (*NIA*; considered to be under neutral selection) and the cDNA sequence of *DFR* (a single gene [*pallida*] that is linked to the *Rosea* locus) from the *ros^{col}* line, other *A. majus* accessions, and other *Antirrhinum* species. The *NIA* and *DFR* sequences from *ros^{col}* cluster with all of the other *A. majus* accessions, whereas the *Ros1* gene sequence from *ros^{col}* clusters with *Ros1* from *Antirrhinum siculum*, and that from *ros^{dor}* clusters with *Ros1* from *A. molle* and *A. meonanthemum* (Venail, 2005).

This small family of MYB-related genes controls the pattern and intensity of pigmentation of flowers. Neither the *ros^{col}* nor the *ros^{dor}* mutation eliminates pigmentation of the vegetative tissues, although the stem tissue of the *ros^{col}* mutant lacks anthocyanin pigmentation when plants are grown in the field. This suggests that *Ros1* is responsible for the induction of anthocyanin biosynthesis in stem tissues as well as inducing the strong production of magenta cyanidin in flowers. In *ros^{col}* plants, the abaxial (ventral) epidermis of the leaves is pigmented when plants are grown in the field, suggesting that color production there is either under the control of *Ros2* or under the control of another MYB-like gene that is not involved in floral pigmentation. The small family of MYB-like genes controlling floral pigmentation in *A. majus* appears to have resulted from successive duplications, one producing the ancestral versions of *Ve* and *Ros1/Ros2*, and the second, which occurred intrachromosomally, giving rise to *Ros1* and *Ros2*. Similar recent intrachromosomal amplifications have occurred for the orthologous family of genes in *Arabidopsis* (*PAP1*, *PAP2*, *MYB113*, and *MYB114*) (Stracke et al., 2001), in grape (*MYBA1* and *MYBA2*) (Kobayashi et al., 2004, 2005), and in potato and tomato (De Jong et al., 2004). In *Petunia*, *AN2* is reportedly structurally very similar to *AN4*, which regulates pigment production in anthers (Spelt et al., 2000; Koes et al., 2005), although these duplicate genes are not linked. What is perhaps even more remarkable is that variation in these MYB-like genes forms the basis for all of the variations in color pattern and intensity between different species that have been investigated.

This has already been demonstrated for the difference between the white flowers of *Petunia axillaris* and the purple flowers of *Petunia integrifolia*, in which loss of activity at the *AN2* locus underpins the acyanic coloring of *P. axillaris* (Quattrocchio et al., 1999).

Here, we have shown that it is differences in the activity of the three MYB-like genes controlling floral pigmentation that underpin the flower color and pattern differences in at least six species within the genus *Antirrhinum*. The number of genes that could contribute to variations in color patterning and intensity is large: all of the structural genes committed to flavonoid biosynthesis, which in *Antirrhinum* amounts to 10 (*CHS*, *CHI*, *F3H*, *F3'H*, *DFR*, *ANS*, *UFGT*, *RT*, *GST*, and *AT*), and the genes encoding bHLH proteins involved in regulating floral pigmentation (*Del* and *Mut*) (Stubbe, 1966; Goodrich et al., 1992; P. Piazza, C. Tonelli, and C. Martin, unpublished data). Although Stubbe (1966) reported that *A. latifolium* differs from *A. majus* in the activity of the *incolorata* locus (which encodes F3H), we did not find any evidence for this in the two accessions of *A. latifolium* (from Marseilles and Pyrea) we examined. This difference is likely to be attributable to differences between the individual accessions that were studied in each case. It was surprising that all of the variation in pigmentation color and pattern that we examined in the genus *Antirrhinum* could be attributed to variation in the activity of the three MYB genes, *Ros1*, *Ros2*, and *Ve*. One possible explanation is that the full-red color of *A. majus* flowers was derived from an ancestor with very pale floral pigmentation, and all of the other palely pigmented members of the genus *Antirrhinum* might carry the same ancestral, low-activity *ros* allele. Investigation of this possibility would require a robust molecular phylogeny, which is not currently available for the European species, largely because the high degree of sequence similarity among species for the markers investigated to date makes resolution difficult, and also because there are significant levels of gene flow between sympatric populations as a result of the cross-fertility of the species (Oyama and Baum, 2004; Vargas et al., 2004; Mateu-Andres and de Paco, 2005; Venail, 2005). However, such an explanation of why color variation derives from variations in the activity of the MYB genes in the genus *Antirrhinum* is unlikely to be correct, because each species accession carries at least one distinct *Ros* allele, as judged by restriction fragment length polymorphisms with several different enzymes (Venail, 2005), and, although palely pigmented, the patterns of anthocyanin production in *A. graniticum*, *A. molle*, *A. mollissimum*, *A. latifolium*, and *A. meonanthemum* are quite distinct, when examined closely. Indeed, the *ros* alleles in *A. graniticum*, *A. molle*, and *A. mollissimum* are fully recessive to *Ros*⁺ from *A. majus*, whereas the *ros* alleles from *A. latifolium* and *A. meonanthemum* are semidominant to *Ros*⁺. We have found that there is also significant variation at the *Ve* locus, with *A. graniticum* lacking *Ve* activity and two independent *A. majus* accessions being polymorphic for *Ve* activity.

The fact that variation in anthocyanin production in flowers is attributable to variation in MYB gene activity in both *Antirrhinum* and *Petunia* (Quattrocchio et al., 1999), in berry skin color in grape (Kobayashi et al., 2004, 2005), and in tuber color in potato (De Jong et al., 2004) suggests that the same route for generating pattern and color diversity has been followed independently on a

number of occasions. In contrast with these results, examination of the sequences encoding the variable C-terminal domain of an equivalent protein, *myb1*, in different *Ipomoea* species suggested neutral variation, leading to the conclusion that rapid evolution of *Ipomoea myb1* has not contributed to differences in floral hue and color patterning among *Ipomoea* species (Chang et al., 2005). However, that study did not investigate possible differences in the level or patterning of *Ipomoea myb1* expression in relation to differences in pigmentation. In addition, the *Ipomoea* species selected for comparison in this study differed principally in the type of anthocyanin they accumulate, a trait less likely to be determined by regulatory gene activity than pigmentation intensity and patterning. Interestingly, an earlier investigation concluded that most of the differences in color between species in the genus *Ipomoea* were attributable to differences in the expression (i.e., the regulation) of the anthocyanin biosynthetic genes (Durbin et al., 2003), suggesting that variation in regulatory gene activity is central to variation in color intensity and patterning within this genus as well.

Is there something special about the activity of the MYB proteins in the regulation of anthocyanin biosynthesis that makes them particularly suitable for the generation of diversity? Clearly, gene duplication and divergence in the patterns of expression of the encoded regulatory proteins offer a rapid means of generating differences in patterns and intensity of pigmentation, which require a significant number of enzymes for their synthesis. However, the evolutionary emphasis on variation in the regulation of MYB gene activity remains puzzling.

In *Arabidopsis*, a complex of MYB, bHLH, and WD repeat proteins regulates not only anthocyanin biosynthesis but also condensed tannin biosynthesis, trichome initiation, and non-root-hair cell specification (Zhang et al., 2003; Serna, 2004; Broun, 2005; Ramsay and Glover, 2005; Lepiniec et al., 2006). A similar complex probably also regulates seed coat mucilage production. In these cases, the WD repeat protein (TTG1) is the same in all of the different functional complexes, and the bHLH proteins are flexible in their participation, GLABRA3 (GL3) and ENHANCER OF GLABRA3 (EGL3) being thought to be involved in non-root-hair cell specification, trichome initiation, and anthocyanin production (Payne et al., 2000; Zhang et al., 2003), and TT8 being involved in both condensed tannin and anthocyanin production (Nesi et al., 2000; Zhang et al., 2003). A similar diversification of functions has been described for the AN1 bHLH protein in *Petunia*, which controls both anthocyanin formation and seed coat morphology (Spelt et al., 2002). Functional specificity is provided in all of these complexes by the participation of specific MYB proteins, although, in the case of non-root-hair cell specification and trichome initiation, the MYB proteins involved, WER and GL1, are functionally interchangeable (Lee and Schiefelbein, 2001) and specificity must be provided by the cellular context in which the proteins are normally active. The specific roles of MYB proteins in multifunctional MYB-bHLH-WD repeat complexes may mean that it is their activity that dictates the net activity of the regulatory complex in controlling any specific target pathway. If the activity of the MYB-related proteins is generally the component that defines the intensity and/or pattern of anthocyanin production, plants may be particularly sensitive to the dosage of the genes encoding these proteins.

Such sensitivity might favor repeated, selective duplication of these genes to generate variation in the intensity and patterning of color in plant tissues.

METHODS

Plant Material

Antirrhinum majus mutants *ros^{col}* and *ros^{dor}* were obtained as standard genetic stocks from the germplasm collection at the Institut für Kulturpflanzenforschung in Gatersleben, Germany. These stocks were crossed to a wild-type, full-red stock (Jl:522), and the mutants were reselected in the F2 generation. The lines carrying these mutations were maintained subsequently by self-pollination for more than five generations. Line Jl:522 is a wild-type revertant from an unstable *nivea^{recurrens}* mutant (Martin et al., 1991). The dominant *Ve⁺* allele of *A. majus* was identified in F2 populations from crosses between the *decipiens* mutant of *A. majus* (from the germplasm collection at the Institut für Kulturpflanzenforschung) and *ros^{col}* and *ros^{dor}*. *Ve⁺* is very tightly linked to the *decipiens* mutant allele, and no recombinants between the two loci have been found. Because the *decipiens* mutation affects the development of petals, the *Ve⁺* allele has been maintained as a heterozygote (*Ve⁺/ve⁻*) in both *ros^{col}* and *ros^{dor}* backgrounds. Comparisons of biosynthetic gene transcript levels were made on RNA from flowers pooled from individuals of the same phenotype segregating in F2 populations of the wild type \times *ros^{col}* and *ros^{dor}* *Ve⁺ \times ros^{dor}*.

The origins of the different *Antirrhinum* species accessions used in this work were *A. majus* subsp. *majus* var. *majus* (Toulouse and Barcelona) and *A. latifolium* (Marseilles and Pyrea), all from the germplasm collection at the Institut für Kulturpflanzenforschung, and *A. graniticum*, *A. molle*, *A. mollissimum*, *A. meonanthemum*, *A. barrelieri*, and *A. australe*, which were collected by R.K. Oyama in Spain, vouchers of which are deposited at the Herbarium of the Arnold Arboretum of Harvard University.

RNA Extraction and Gel Electrophoresis

Total RNA was extracted by freezing tissue in liquid nitrogen and then grinding it to a fine powder, which was then added to extraction buffer (150 mM LiCl, 50 mM Tris-HCl, pH 9, 5 mM EDTA, pH 8.0, and 5% [w/v] SDS). Two phenol-chloroform extractions were performed on the extract, followed by a chloroform extraction. The RNA in the resulting aqueous phase was precipitated overnight at 4°C by the addition of 8 M LiCl to a final concentration of 2 M LiCl. The precipitate was resuspended in TE buffer (10 mM Tris-HCl, pH 8.0, and 1 mM EDTA). Two further rounds of precipitation in 2 M LiCl were performed. Samples were redissolved in TE buffer. Poly(A)⁺ RNA was isolated using poly(A)⁺ RNA purification kits (Amersham Pharmacia Biotech). RNA gel electrophoresis was performed as described by Martin et al. (1991).

First-Strand cDNA Synthesis

First-strand cDNA was made using a cDNA synthesis kit (Amersham) according to the manufacturer's instructions, except that the cDNA was primed with the dT₁₇ adaptor sequence (Frohmann et al., 1988). Ten micrograms of total RNA was used for each reaction, and the cDNA was diluted to a final volume of 1 mL with sterile, distilled water. Samples of 10 μ L (~200 ng of cDNA template) were used for 3' RACE PCR.

3' RACE PCR

Reactions were conducted in a 100- μ L final volume including 200 ng of template cDNA, 1 \times AmpliTaq buffer (Perkin-Elmer), 50 μ M deoxynucleotide triphosphates, 50 nM of each primer, and 0.5 μ L (2.5 units)

of AmpliTaq polymerase (Perkin-Elmer). The primers used for *Ros1* were G1709 (forward, 5'-AAAAGCTGCAGACTTAGGTGGTTGAATTATC-TAAAGCC-3') and the adaptor sequence (reverse, 5'-GACTCGAGCGA-CATCGAT-3') (Frohmann et al., 1988), and those used for *Ros2* were K17 (forward, 5'-TAGTGCATATGCTAAACGCAATGC-3') and the adaptor sequence (reverse, 5'-GACTCGAGCGACATCGAT-3') (Frohmann et al., 1988). The PCR conditions were 40 cycles of 94°C for 1 s, 94°C for 40 s, 55°C for 2 min, 55°C for 1 s, 72°C for 1 min, and 72°C for 3 min, followed by 10 min of final extension at 72°C.

RT-PCR Amplification of *DFR* cDNA

cDNA was amplified by the method of Frohmann et al. (1988) using the primers DFR-F (5'-ATGAGTCCCACCTTCACTAAATACGAGTTCCGA-AAC-3') and DFR-R (5'-CTAGATTCTGCCATCAGTATGATCGTTTG-CAATGTC-3') for 40 cycles. DNA was transferred by blotting to nitrocellulose filters and hybridized with an *EcoRI*-*Bam*HI fragment of genomic DNA from the *Pallida* (*DFR*) locus of *A. majus* (Coen et al., 1986).

Large-Scale DNA Extractions

Twenty to thirty grams of young leaves were collected, frozen in liquid nitrogen, and used directly or stored at -70°C. The frozen material was ground to a fine powder and transferred to DNA extraction buffer (0.1 M EDTA, 3 \times SSC [1 \times SSC is 0.15 M NaCl and 0.015 M sodium citrate], 0.1 M sodium diethyldithiocarbamate, and 1% SDS). Samples were then placed at 37°C for 5 to 10 min to let the material thaw. The homogenate was extracted with phenol:chloroform (1:1) two times, and then once with chloroform alone. DNA was precipitated by the addition of two volumes of 90% ethanol to the aqueous phase. The pellet was resuspended in 9 mL of TE buffer, pH 8, and exactly 1 g/mL cesium chloride was added to the resuspended DNA solution. The gradients were centrifuged at 65,000 rpm at 15°C for 16 to 20 h, after which time the tubes were visualized under UV light and the DNA, visible as a single fluorescent band, was removed with a needle and hypodermic syringe. The ethidium bromide was removed with salt-saturated isopropanol. The DNA was precipitated with two volumes of 100% ethanol. The pellets were washed with 70% ethanol and resuspended in 500 μ L of TE buffer, pH 8.

PCR Amplification of Genomic DNA

Reactions were performed in a total volume of 100 μ L, containing 5 μ L (~200 ng) of genomic DNA as a template, 50 nM primer, 250 μ M deoxynucleotide triphosphates, 1 \times AmpliTaq buffer (Perkin-Elmer), and 0.5 μ L (2.5 units) of AmpliTaq polymerase (Perkin-Elmer). Thirty-five cycles of amplification were performed under the following conditions: 94°C for 30 s, 50°C for 30 s, and 72°C for 1.5 min, followed by 10 min of final extension at 72°C. The enzyme AmpliTaq and its buffer were obtained from Perkin-Elmer. The primers used for *Ros2* were J19 (forward, 5'-CCGAGCTTCGGACCTTCAATGGATTG-3'), J21 (forward, 5'-CCACTTTTATGCGTCACTACACATGTCATAT-3'), and J22 (reverse, 5'-CTATGTTTGCAAACGTTTATGGTTG-3').

Oligolabeling of DNA Probes

The templates used for the synthesis of the DNA probes were PCR fragments amplified from plasmids containing the clones of *Ros1*, *Ros2*, *Ve*, *CHS*, *CHI*, *F3H*, *F3'H*, *FLS*, *DFR*, *ANS*, *UFGT*, and *AT* cDNAs cloned in pBluescript SK+ (Stratagene) or pGEM-T easy (Promega), or restriction fragments from the same plasmids. Radioactively labeled probes were produced using the *rediprime* II random prime labeling kit (Amersham Pharmacia Biotech), and newly synthesized DNA was made radioactive by replacing nonradioactive dCTP with [α -³²P]dCTP. Reactions were

fractionated on a drip column of Sephadex G-50 in TE buffer to separate the labeled DNA from the free nucleotides and boiled to denature the DNA before hybridization.

Transfer of Nucleic Acids to Membranes

DNA gel blotting followed the procedure of Maniatis et al. (1982). Twenty microliters of 3' RACE PCR product or 5 to 10 μ g of digested genomic DNA was loaded onto agarose gels in TBE buffer (0.09 M Tris-HCl, 0.09 M boric acid, and 2 mM EDTA) and separated by electrophoresis. After staining with ethidium bromide and photography over a UV light trans-illuminator, gels were treated with 0.25 M HCl to depurinate the DNA, then with denaturation buffer (0.5 M NaOH and 1.5 M NaCl), and finally with neutralization buffer (1 M Tris-HCl, pH 8.0, and 1.5 M NaCl). Gels were blotted onto nitrocellulose membranes (Protran BA 85; Schleicher and Schuell) overnight. RNA gels were blotted onto nitrocellulose directly in 10 \times SSC overnight. Filters were then baked in a vacuum oven at 80°C for 2 h before use.

Hybridization of Filters

Filters were prehybridized at 65°C for 2 h in prehybridization solution (6 \times SSC, 0.2% polyvinylpyrrolidone [molecular weight 40,000], 0.2% Ficoll [molecular weight 40,000], and 0.1% [w/v] SDS), supplemented with 50 μ g/mL sonicated and boiled salmon sperm DNA, and hybridized overnight with denatured, radioactive probes at 65°C (high stringency) or 55°C (low stringency) in hybridization solution (3 \times SSC, 0.02% polyvinylpyrrolidone [molecular weight 40,000], 0.02% Ficoll [molecular weight 40,000], and 0.1% [w/v] SDS), supplemented with 50 μ g/mL denatured salmon sperm DNA. They were then washed twice at 55°C for 2 h in low-stringency solution (3 \times SSC and 0.5% SDS) for low-stringency washes or twice for 20 min in high-stringency solution (0.1 \times SSC and 0.5% SDS) at 65°C for high-stringency washes. Filters were air-dried, wrapped in Saran wrap plastic film, and exposed to x-ray film (Kodak Biomax MS with Biomax imaging screens) at -70°C.

Particle Bombardment Experiments

A. majus plants of the genotype *ros^{dar}* were grown in the greenhouse, conditions under which anthocyanin did not form on the petal lobes. Bombardment was conducted using a particle inflow helium gun based on the design of Vain et al. (1993), but modified to use a polycarbonate desiccator (Nalgene) as the chamber. The lobe tissue from young, just-opened flowers was dissected and sterilized in 10% bleach containing one drop of Tween 20 per 100 mL, for between 10 and 15 min, and rinsed in sterilized, distilled water. Plasmid DNA (20 μ g) was precipitated onto 5 mg gold particles (1.0 μ m diameter) through the addition of 50 μ L of 2.5 M CaCl_2 and 20 μ L of 100 mM spermidine. After precipitation, 90 μ L of supernatant was discarded. Gold particles were prepared immediately before use.

For bombardment, petal tissue was placed on an empty Petri dish or on 0.5 \times Murashige and Skoog (1962) medium plus 7.5% agar (MS medium) in a Petri dish, within the desiccator in the gun range of 120 to 160 mm. Tissue was bombarded with 4 μ L of gold suspension using a 50-ms burst of helium at a pressure of 600 kPa within a vacuum of -95 kPa. Each sample was bombarded between one and three times. After bombardment, tissue was incubated on MS medium at 20°C in a 16-h-light/8-h-dark photoperiod with 35 $\text{mmol}\cdot\text{m}^{-2}\cdot\text{s}^{-1}$ cool-white fluorescent light. Tissue was observed for anthocyanin production after 2 d.

Histochemical staining for GUS activity was performed by incubating petal tissue in 50 mM phosphate buffer, pH 7.0, containing 0.35 mg/mL 5-bromo-4-chloro-3-indolyl- β -glucuronic acid substrate. Tissue was incubated in the dark at 37°C for 24 h before examination for staining.

Phylogenetic Methods

Protein sequences were manually aligned using MacClade 4.08 (D.R. Maddison and W.P. Maddison, Sinauer Associates). Phylogenetic analysis was performed with PAUP* 4.0b10 (Swofford, 2001), using only the MYB domain of each protein (see Supplemental Figure 1 online) (Kranz et al., 1998). An optimal tree according to the distance criterion (minimum evolution; mean character difference) was obtained with a heuristic search (tree bisection reconnection). One thousand bootstrapped data sets were used to estimate the confidence of each tree clade.

Accession Numbers

Sequence data from this article can be found in the GenBank/EMBL data libraries under accession numbers DQ275529 (*Ros1* cDNA), DQ275530 (*Ros2* cDNA), DQ275531 (*Ve* cDNA), DQ272591 (*FLS* cDNA from *A. majus*), and DQ272592 (*F3'H* cDNA from *A. majus*).

Supplemental Data

The following materials are available in the online version of this article.

Supplemental Figure 1. Alignment of Sequences of MYB-Related Transcription Factors Controlling Anthocyanin Biosynthesis in Different Plant Species.

Supplemental Figure 2. Phenotypes from Genetic Analysis of *A. graniticum*, *A. meonanthemum*, and *A. latifolium*.

Supplemental Figure 3. Expression of the Gene Encoding DFR in Flowers with Different Phenotypes Shown by Saturating RT-PCR.

Supplemental Table 1. Genetic Analysis of Flower Color and Pattern in the Genus *Antirrhinum*.

ACKNOWLEDGMENTS

We thank Rosemary Carpenter for providing seed of the species accessions from the Institut für Kulturpflanzenforschung and for advice on growth, selfing, and crossing these lines; Emma Conklin for technical assistance in part of this work; Hans Sommer for the *Antirrhinum* genomic library; Rachael Lewis (John Innes Centre) for researching many of the more difficult references; the New Zealand Institute for Crop and Food Research for sponsoring K.S.; the Marsden Fund, New Zealand for supporting K.S., Y.S., and C.M.; the Foundation for Research, Science, and Technology, New Zealand for supporting K.S. and K.D.; the European Union FP5 program for sponsorship through the Profood project (QLK1-CT-2001-01080); the Core Strategic Grant from the Biotechnology and Biological Science Research Council to the John Innes Centre for supporting C.M. and S.M.; and the Marshall Sheffield Foundation for support of R.O. during the course of this work.

Received November 5, 2005; revised January 10, 2006; accepted February 7, 2006; published March 10, 2006.

REFERENCES

- Almeida, J., Carpenter, R., Robbins, T.P., Martin, C., and Coen, E.S. (1989). Genetic interactions underlying flower colour patterns in *Antirrhinum majus*. *Genes Dev.* **3**, 1758-1767.
- Baur, E. (1910a). Vererbungs- und Bastardierungsversuche mit *Antirrhinum*. *Z. Indukt. Abstammungs. Vererbungs.* **3**, 34-98.

- Baur, E. (1910b). Untersuchungen über die Vererbung von Chromatophorenmerkmalen bei *Melandrium*, *Antirrhinum* und *Aquilegia*. Z. Indukt. Abstammungs. Vererbungs. 4, 81–102.
- Bey, M., Stuber, K., Fellenberg, K., Schwarz-Sommer, Z., Sommer, H., Saedler, H., and Zachgo, S. (2004). Characterization of *Antirrhinum* petal development and identification of target genes of the class B MADS box gene *DEFICIENS*. Plant Cell 16, 3197–3215.
- Bollmann, J., Carpenter, R., and Coen, E.S. (1991). Allelic interactions at the *nivea* locus of *Antirrhinum*. Plant Cell 3, 1327–1336.
- Borevitz, J.O., Xia, Y., Blount, J., Dixon, R.A., and Lamb, C.J. (2000). Activation tagging identifies a conserved MYB regulator of phenylpropanoid biosynthesis. Plant Cell 12, 2383–2394.
- Borovsky, Y., Oren-Shamir, M., Ovadia, R., De Jong, W., and Paran, I. (2004). The A locus that controls anthocyanin accumulation in pepper encodes a MYB transcription factor homologous to *Anthocyanin2* of *Petunia*. Theor. Appl. Genet. 109, 23–29.
- Broun, P. (2005). Transcriptional control of flavonoid biosynthesis: A complex network of conserved regulators involved in multiple aspects of differentiation in Arabidopsis. Curr. Opin. Plant Biol. 8, 272–279.
- Carey, C.C., Strahle, J.T., Selinger, D.A., and Chandler, V.L. (2004). Mutations in the *pale aleurone color1* regulatory gene of the *Zea mays* anthocyanin pathway have distinct phenotypes relative to the functionally similar *TRANSPARENT TESTA GLABRA1* gene in *Arabidopsis thaliana*. Plant Cell 16, 450–464.
- Chandler, V.L., Radicella, J.P., Robbins, T.P., Chen, J., and Turks, D. (1989). Two regulating genes of the maize anthocyanin pathway are homologous: Isolation of *B* using *R* genomic sequences. Plant Cell 1, 1175–1183.
- Chang, S.-M., Lu, Y., and Rausher, M.D. (2005). Neutral evolution of the non-binding region of the anthocyanin regulatory gene *Ipmyb1* in *Ipomoea*. Genetics 170, 1967–1978.
- Coen, E.S., and Carpenter, R. (1988). A semi-dominant allele, *niv-525*, acts in trans to inhibit expression of its wild type homologue in *Antirrhinum majus*. EMBO J. 7, 877–883.
- Coen, E.S., Carpenter, R., and Martin, C. (1986). Transposable elements generate novel spatial patterns of gene expression in *Antirrhinum majus*. Cell 47, 285–296.
- Cone, K.C., Burr, F.A., and Burr, B. (1986). Molecular analysis of the maize anthocyanin regulatory locus *C1*. Proc. Natl. Acad. Sci. USA 83, 9631–9635.
- Cone, K.C., Cocciolone, S.M., Burr, F.A., and Burr, B. (1993). Maize anthocyanin regulatory gene *pl* is a duplicate of *c1* that functions in the plant. Plant Cell 5, 1795–1805.
- Consonni, G., Geuna, F., Gavazzi, G., and Tonelli, C. (1993). Molecular homology among members of the *R*-gene family in maize. Plant J. 3, 335–346.
- Consonni, G., Viotti, A., Dellaporta, S.L., and Tonelli, C. (1992). cDNA nucleotide sequence of *Sn*, a regulatory gene in maize. Nucleic Acids Res. 20, 373.
- De Jong, W.S., Eannetta, N.T., De Jong, D.M., and Bodis, M. (2004). Candidate gene analysis of anthocyanin pigmentation loci in the *Solanaceae*. Theor. Appl. Genet. 108, 423–432.
- Della Vedova, C.B., Lorbietke, R., Kirsch, H., Schulte, M.B., Scheets, K., Borchert, L.M., Scheffler, B.E., Wienand, U., Cone, K.C., and Birchler, J.A. (2005). The dominant inhibitory chalcone synthase allele *C2-Idf* (*Inhibitor diffuse*) from *Zea mays* acts via an endogenous RNA silencing mechanism. Genetics 170, 1989–2002.
- de Vetten, N., Quattrocchio, F., Mol, J., and Koes, R. (1997). The *an11* locus controlling flower pigmentation in *petunia* encodes a novel WD-repeat protein conserved in yeast, plants and animals. Genes Dev. 11, 1422–1434.
- Durbin, M.L., Lundy, K.E., Morrell, P.L., Torres-Martinez, C.L., and Clegg, M.T. (2003). Genes that determine flower color: The role of regulatory changes in the evolution of phenotypic adaptations. Mol. Phylogenet. Evol. 29, 507–518.
- Frohmann, M.A., Dush, M.K., and Martin, G.R. (1988). Rapid production of full length cDNAs from rare transcripts—Amplification using a single gene-specific oligonucleotide primer. Proc. Natl. Acad. Sci. USA 85, 8998–9002.
- Goff, S.A., Cone, K.C., and Chandler, V.L. (1992). Functional analysis of the transcriptional activator encoded by the maize *B* gene: Evidence for a direct functional interaction between two classes of regulatory proteins. Genes Dev. 6, 864–875.
- Gong, Z.Z., Yamagishi, E., Yamazaki, M., and Saito, K. (1999). A constitutively expressed Myc-like gene involved in anthocyanin biosynthesis from *Perilla frutescens*: Molecular characterisation, heterologous expression in transgenic plants and transactivation in yeast cells. Plant Mol. Biol. 41, 33–44.
- Goodrich, J., Carpenter, R., and Coen, E.S. (1992). A common gene regulates pigmentation pattern in diverse plant species. Cell 68, 955–964.
- Grotewold, E., Sainz, M.B., Tagliani, L., Hernandez, J.M., Bowen, B., and Chandler, V.L. (2000). Identification of the residues in the Myb domain of maize C1 that specify the interaction with the bHLH cofactor R. Proc. Natl. Acad. Sci. USA 97, 13579–13584.
- Harbourne, J.B., and Smith, D.M. (1978). Anthochlors and other flavonoids as honey guides in the Compositae. Biochem. Syst. Ecol. 6, 287–291.
- Hodges, S.A., and Arnold, M.L. (1994). Floral and ecological isolation between *Aquilegia formosa* and *Aquilegia pubescens*. Proc. Natl. Acad. Sci. USA 91, 2493–2496.
- Jackson, D., Roberts, K., and Martin, C. (1992). Temporal and spatial control of expression of anthocyanin biosynthetic genes in developing flowers of *Antirrhinum majus*. Plant J. 2, 425–434.
- Kobayashi, S., Goto-Yamamoto, N., and Hirochika, K. (2004). Retrotransposon-induced mutations in grape skin color. Science 304, 982.
- Kobayashi, S., Ishimaru, M., Hiraoka, K., and Honda, C. (2002). Myb-related genes of the Kyoho grape (*Vitis lambrusca*) regulate anthocyanin biosynthesis. Planta 215, 924–933.
- Kobayashi, S., Yamamoto, N.G., and Hirochika, H. (2005). Association of *VvmybA1* gene expression with anthocyanin production in grape (*Vitis vinifera*) skin-color mutants. J. Jpn. Soc. Hortic. Sci. 74, 196–203.
- Koes, R., Verweij, W., and Quattrocchio, F. (2005). Flavonoids: A colorful model for the regulation and evolution of biochemical pathways. Trends Plant Sci. 10, 236–242.
- Kranz, H.D., et al. (1998). Towards functional characterisation of the members of the *R2R3-MYB* gene family from *Arabidopsis thaliana*. Plant J. 16, 263–276.
- Kuckuck, H., and Schick, R. (1930). Die Erbfaktoren bei *Antirrhinum majus* und ihre Bezeichnung. Z. Indukt. Abstammungs. Vererbungs. 56, 51–83.
- Lee, M.M., and Schiefelbein, J. (2001). Developmentally distinct MYB genes encode functionally equivalent proteins in Arabidopsis. Development 128, 1539–1546.
- Lepiniec, L., Debeaujon, I., Routaboul, J.M., Baudry, A., Pourcel, L., Nesi, N., and Caboche, M. (2006). Genetics and biochemistry of seed flavonoids. Annu. Rev. Plant Biol. 57, 405–430.
- Lonig, W.E., and Saedler, H. (1997). Plant transposons: Contributors to evolution? Gene 205, 245–253.
- Ludwig, S.R., Habera, L.F., Dellaporta, S.L., and Wessler, S.R. (1989). *Lc*, a member of the maize *R* gene family responsible for tissue-specific anthocyanin production, encodes a protein similar to transcriptional activators and contains the *myc* homology region. Proc. Natl. Acad. Sci. USA 86, 849–851.

- Lunau, K., Wacht, S., and Chittka, L. (1996). Colour choices of naïve bumble bees and their implications for colour perception. *J. Comp. Physiol. [A]* **178**, 477–489.
- Maniatis, T., Fritsch, E.F., and Sambrook, J. (1982). *Molecular Cloning: A Laboratory Manual*. (Cold Spring Harbor, NY: Cold Spring Harbor Laboratory Press).
- Martin, C., Carpenter, R., Coen, E.S., and Gerats, T. (1987). The control of floral pigmentation in *Antirrhinum majus*. In *Developmental Mutants in Higher Plants*, H. Thomas and D. Grierson, eds (Cambridge, UK: Cambridge University Press), pp. 19–52.
- Martin, C., Carpenter, R., Sommer, H., Saedler, H., and Coen, E.S. (1985). Molecular analysis of instability in flower pigmentation in *Antirrhinum majus*, following isolation of the *pallida* locus by transposon tagging. *EMBO J.* **4**, 1625–1630.
- Martin, C., and Gerats, T. (1993). The control of pigment biosynthesis genes during petal development. *Plant Cell* **5**, 1253–1264.
- Martin, C., and Lister, C. (1989). Genome juggling by transposons: Tam3-induced rearrangements in *Antirrhinum majus*. *Dev. Genet.* **10**, 438–451.
- Martin, C., Prescott, A., Mackay, S., Bartlett, J., and Vrijlandt, E. (1991). Control of anthocyanin biosynthesis in flowers of *Antirrhinum majus*. *Plant J.* **1**, 37–49.
- Mateu-Andres, I., and de Paco, L. (2005). Allozymic differentiation of the *Antirrhinum majus* and *A. siculum* species groups. *Ann. Bot. (Lond.)* **95**, 465–473.
- Mathews, H., Clendennen, S.K., Caldwell, C.G., Liu, X.L., Connors, K., Matheis, N., Schuster, D.K., Menasco, D.J., Wagoner, W., Lightner, J., and Wagner, D.R. (2003). Activation tagging in tomato identifies a transcriptional regulator of anthocyanin biosynthesis, modification, and transport. *Plant Cell* **15**, 1689–1703.
- Molina, C., and Grotewold, E. (2005). Genome wide analysis of Arabidopsis core promoters. *BMC Genomics* **6**, 25.
- Murashige, T., and Skoog, F. (1962). A revised medium for rapid growth and bioassays with tobacco tissue cultures. *Physiol. Plant.* **15**, 473–478.
- Nesi, N., Debeaujon, I., Jond, C., Pelletier, G., Caboche, M., and Lepiniec, L. (2000). The *TT8* gene encodes a basic helix-loop-helix domain protein required for expression of *DFR* and *BAN* genes in Arabidopsis siliques. *Plant Cell* **12**, 1863–1878.
- Oyama, R.K. (2002). *Pollinator-Mediated Reproductive Isolation and Speciation in Antirrhinum (Veronicaaceae)*. PhD dissertation (Cambridge, MA: Harvard University).
- Oyama, R.K., and Baum, D.A. (2004). Phylogenetic relationships of North American *Antirrhinum* (Veronicaaceae). *Am. J. Bot.* **91**, 918–925.
- Park, K.-I., Choi, J.-D., Hoshino, A., Morita, Y., and Iida, S. (2004). An intragenic tandem duplication in a transcriptional regulatory gene for anthocyanin biosynthesis confers pale colored flowers and seeds with fine spots in *Ipomoea tricolor*. *Plant J.* **38**, 840–849.
- Payne, C.T., Zhang, F., and Lloyd, A.M. (2000). *GL3* encodes a bHLH protein that regulates trichome development in Arabidopsis through interaction with GL1 and TTG1. *Genetics* **156**, 1349–1362.
- Paz-Ares, J., Ghosal, D., Wienand, U., Peterson, P.A., and Saedler, H. (1987). The regulatory *C1* locus of *Zea mays* encodes a protein with homology to *myb* protooncogene products and with structural similarities to transcriptional activators. *EMBO J.* **6**, 3553–3558.
- Paz Ares, J., Wienand, U., Peterson, P.A., and Saedler, H. (1986). Molecular-cloning of the *C* locus of *Zea mays*—A locus regulating the anthocyanin pathway. *EMBO J.* **5**, 829–833.
- Penny, J.H.J. (1983). Nectar guide color contrast—A possible relationship with pollination strategy. *New Phytol.* **95**, 707–721.
- Pilu, R., Piazza, P., Petroni, K., Ronchi, A., Martin, C., and Tonelli, C. (2003). *pl-bol3*, a complex allele of the anthocyanin regulatory *pl1* locus that arose in a naturally occurring maize population. *Plant J.* **36**, 510–521.
- Quattrocchio, F. (1994). *Regulatory Genes Controlling Flower Pigmentation in Petunia hybrida*. PhD dissertation (Amsterdam: Vrije Universiteit).
- Quattrocchio, F., Wing, J.F., van der Woude, K., Mol, J.N.M., and Koes, R. (1998). Analysis of bHLH and MYB domain proteins: Species specific regulatory differences are caused by divergent evolution of target anthocyanin genes. *Plant J.* **13**, 475–488.
- Quattrocchio, F., Wing, J.F., van der Woude, K., Souer, E., de Vetten, N., Mol, J.N.M., and Koes, R. (1999). Molecular analysis of the *anthocyanin2* gene of petunia and its role in the evolution of flower color. *Plant Cell* **11**, 1433–1444.
- Ramsay, N.A., and Glover, B.J. (2005). MYB-bHLH-WD40 protein complex and the evolution of cellular diversity. *Trends Plant Sci.* **10**, 63–70.
- Robbins, T.P., Carpenter, R., and Coen, E.S. (1989). A chromosomal rearrangement suggests that donor and recipient sites are associated during Tam3 transposition in *Antirrhinum majus*. *EMBO J.* **8**, 5–13.
- Sainz, M.B., Goff, S.A., and Chandler, V.L. (1997a). Extensive mutagenesis of a transcriptional activation domain identifies single hydrophobic and acidic amino acids important for activation in vivo. *Mol. Cell. Biol.* **17**, 115–122.
- Sainz, M.B., Grotewold, E., and Chandler, V.L. (1997b). Evidence for direct activation of an anthocyanin promoter by the maize C1 protein and comparison of DNA binding by related Myb domain proteins. *Plant Cell* **9**, 611–625.
- Schwinn, K.E. (1999). *Regulation of Anthocyanin Biosynthesis in Antirrhinum majus*. PhD dissertation (Norwich, UK: University of East Anglia).
- Serna, L. (2004). A network of interacting factors triggering different cell fates. *Plant Cell* **16**, 2258–2263.
- Sommer, H., and Saedler, H. (1986). Structure of the chalcone synthase gene of *Antirrhinum majus*. *Mol. Gen. Genet.* **202**, 429–434.
- Sompornpailin, K., Makita, Y., Yamazaki, M., and Saito, K. (2002). A WD-repeat containing putative regulatory protein in anthocyanin biosynthesis in *Perilla frutescens*. *Plant Mol. Biol.* **50**, 485–495.
- Spelt, C., Quattrocchio, F., Mol, J., and Koes, R. (2002). *ANTHOCYANIN1* of petunia controls pigment synthesis, vacuolar pH, and seed coat development by genetically distinct mechanisms. *Plant Cell* **14**, 2121–2135.
- Spelt, C., Quattrocchio, F., Mol, J.N.M., and Koes, R. (2000). *anthocyanin1* of petunia encodes a basic helix-loop-helix protein that directly activates transcription of structural anthocyanin genes. *Plant Cell* **12**, 1619–1631.
- Springob, K., Yamazaki, M., and Saito, K. (2003). Functional characterisation of MYBC05, a putative regulator of anthocyanin biosynthesis in *Perilla frutescens*. *Plant Cell Physiol.* **44** (suppl.), S121.
- Stickland, R.G., and Harrison, B.J. (1974). Precursors and genetic control of pigmentation. I. Induced biosynthesis of pelargonidin, cyanidin and delphinidin in *Antirrhinum majus*. *Heredity* **33**, 108–112.
- Stracke, R., Werber, M., and Weisshaar, B. (2001). The *R2R3-MYB* gene family in *Arabidopsis thaliana*. *Curr. Opin. Plant Biol.* **4**, 447–456.
- Stubbe, H. (1966). *Genetik und Zytologie von Antirrhinum L. sect. Antirrhinum*. (Jena, Germany: VEB Gustav Fischer Verlag).
- Sutton, D.A. (1988). *A Revision of the Tribe Antirrhineae*. (Oxford, UK: Oxford University Press).
- Swofford, D.L. (2001). *PAUP*: Phylogenetic Analysis Using Parsimony*. 4.0b10. (Sunderland, MA: Sinauer Associates).
- Thompson, W.R., Meinwald, J., Aneshanslet, D., and Eisner, T. (1972). Flavonols: Pigments responsible for ultraviolet absorption in nectar guide of flower. *Science* **177**, 528–530.

- Vain, P., Keen, N., Murillo, J., Rathus, C., Nemes, C., and Finer, J.J.** (1993). Development of the particle in-flow gun. *Plant Cell Tissue Organ Cult.* **33**, 237–246.
- Vargas, P., Rossello, J.A., Oyama, R., and Guemes, J.** (2004). Molecular evidence for naturalness of genera in the tribe Antirrhineae (Scrophulariaceae) and three independent evolutionary lineages from the New World and the Old. *Plant Syst. Evol.* **249**, 151–172.
- Venail, J.** (2005). Floral Pigmentation in the Genus *Antirrhinum*. PhD dissertation (Norwich, UK: University of East Anglia).
- Walker, A.R., Davison, P.A., Bolognesi-Winfield, A.C., James, C.M., Srinivasan, N., Blundell, T.L., Esch, J.J., Marks, M.D., and Gray, J.C.** (1999). The *TRANSPARENT TESTA GLABRA1* locus which regulates trichome differentiation and anthocyanin biosynthesis in *Arabidopsis* encodes a WD-40 repeat protein. *Plant Cell* **11**, 1337–1349.
- Waser, N.M., and Price, M.V.** (1983). Pollinator behaviour and natural selection for flower colour in *Delphinium nelsonii*. *Nature* **302**, 422–424.
- Wheldale, M.** (1907). The inheritance of flower colour in *Antirrhinum majus*. *Proc. R. Soc. Lond. B Biol. Sci.* **79**, 288–305.
- Zhang, F., Gonzalez, A., Zhao, M., Payne, C.T., and Lloyd, A.** (2003). A network of redundant bHLH proteins functions in all TTG1-dependent pathways of *Arabidopsis*. *Development* **130**, 4859–4869.
- Zimmermann, I.M., Heim, M.A., Weisshaar, B., and Uhrig, J.F.** (2004). Comprehensive identification of *Arabidopsis thaliana* MYB transcription factors interacting with R/B-like BHLH proteins. *Plant J.* **40**, 22–34.